IOVS Papers in Press. Published on April 7, 2010 as Manuscript iovs.09-4914

Proteomic Analysis of Potential Keratan Sulfate, Chondroitin Sulfate A, and Hyaluronic Acid Molecular Interactions

Abigail H. Conrad[a], Yuntao Zhang[a], Elena S. Tasheva, Gary W. Conrad

Division of Biology, Kansas State University, Manhattan, KS
[a]These authors contributed equally to this work and should be considered equivalent authors.

Running Title: Proteomic analyses of KS, CSA, and HA interactions.

Total word count: 7,764

Funding Acknowledgements: This work was funded by an National Institutes of Health (NIH) Microarray Supplement Grant 3R01EY000952-35S1 to NIH 5R01EY000952, and NIH 2 R01EY000952 to GWC. The content of this paper is solely the responsibility of the authors and does not necessarily represent the official views of the National Eye Institute or the National Institutes of Health.

Corresponding Author: Abigail H. Conrad
Division of Biology
Ackert Hall
Kansas State University
Manhattan, KS 66506-4901
Tel: 785-532-6662
Email: aconrad@ksu.edu

Abstract:

Purpose: Corneal stroma extracellular matrix (ECM) glycosaminoglycans (GAGs) include keratan sulfate (KS), chondroitin sulfate A (CSA), and hyaluronic acid (HA). Embryonic corneal keratocytes and sensory nerve fibers grow and differentiate according to chemical cues they receive from their ECM. This study asks what proteins that might regulate keratocytes or corneal nerve growth cone immigration interact with corneal GAGs.

Method: Biotinylated KS (bKS), CSA (bCSA), and HA (bHA) were prepared, and used in Invitrogen's v4 protoarray to assess their interactions with 8268 proteins and a custom array of 85 extracellular epitopes of nerve growth-related proteins. Surface Plasmon Resonance (SPR) was performed with bKS and SLIT2, and their K_a, K_d, and K_D values determined.

Results: Highly sulfated KS interacted with 217 v4 proteins, including 75 kinases, several membrane or secreted proteins, many cytoskeletal proteins, and many nerve function proteins. CSA interacted with 24 v4 proteins, including 10 kinases and 2 cell surface proteins. HA interacted with 6 v4 proteins, including several ECM-related structural proteins. Of 85 ECM nerve-related epitopes, KS bound 40 proteins, including SLIT, 2 ROBOs, 9 EPHs, 8 Ephrins (EFNs), 8 semaphorins (SEMAs) and 2 nerve growth factor receptors. CSA bound 9 proteins, including ROBO2, 2 EPHs, 1 EFN, 2 SEMAs, and Netrin4. HA bound no ECM nerve-related epitopes. SPR confirmed that KS binds SLIT2 strongly. KS core protein mimecan/osteoglycin bound 15 v4 proteins.

Conclusion: Corneal stromal GAGs bind, and thus could alter the availability or conformation of, many proteins that may influence keratocyte behavior and nerve growth cone behavior in the cornea.

Introduction:

Glycosaminoglycans (GAGs) are long unbranched polysaccharide chains composed of repeating disaccharide units, often either D-glucuronic acid (GlcA), L-iduronic acid (IdoA), or D-Galactose (Gal) linked to either D-N-acetylglucosamine (GlcNAc) or D-N-acetylgalactosamine (GalNAc). One or both sugars can be sulfated. The carboxylate ($–COO^-$) and sulfate ($–SO_4^=$) groups make GAGs highly negatively charged polymers. Most GAG chains are synthesized covalently linked at their reducing end to core proteins, thus forming proteoglycans (PGs). The adult human corneal stroma contains (by weight) 65% keratan sulfate (KS) and 30% chondroitin/dermatan sulfate (CS/DS)[1], first identified as major GAGs of the cornea by Meyer and coworkers[2,3]. Corneal KS chains are attached to core proteins lumican, keratocan, and mimecan/osteoglycin[4,5,6], and corneal CS/DS chains are attached to decorin and biglycan[7,8]. In addition, corneal stromal cells in culture[9], early embryonic corneal endothelial cells[10], and anterior stromal cells in injured adult corneas[11] also make hyaluronic acid (HA), unique among GAGs because it is neither covalently attached to a core protein nor sulfated.

GAGs influence many biological functions, including cell division, differentiation, signal transduction, adhesion, migration, peripheral nerve extension or regeneration, and responses to growth factors[12-16], sometimes affecting cell adhesion and/or proliferation differently in different ECM compositions[17]. In exerting these influences, GAGs interact with proteins in many different ways. Clusters of basic amino acids in BBXB and BBBXXB sequences (B = basic amino acid, X = hydrophilic amino acid) have been proposed as consensus GAG binding sites in some proteins[18]. In other cases, interactions between GAGs and proteins appear to be more directly charge-dependent, either because the degree of sulfation of the GAG determines the strength of

the interaction[19], or because an increase in the number of GAG chains on a core protein increases the interactions of that PG with other proteins[20].

Little is known about the protein interactions of corneal GAGs KS, CSA, and HA. KS, composed of repeating –[3Galβ1-4GlcNAcβ1]- disaccharide units, has an average molecular weight of about 15 kDa. In addition to corneal KS core proteins, KS can also be attached to fibromodulin, aggrecan, and PRELP in cartilage, and to osteoadherin in bone[21]. Although often an ECM component, KS can also be on cell surfaces[22,23], or in the cytosol [24]. KS chains are sulfated to different degrees in different tissues[25], at different stages of development within a given tissue[26], and in different disease states[27]. KS chains bind cardiotoxins CTX A3 and Tgamma[28] and insulin-like growth factor binding protein-2 (IGFBP2)[29]. KS core proteins keratocan and lumican bind CXC chemokine KC during corneal inflammatory response[30]. No binding partners for mimecan/osteoglycin have been reported.

CS is composed of repeating –[4GlcAβ1-3GalNAcβ1**]-** disaccharide units, with sulfate groups covalently attached to C-4 of GalNAc (CSA), C-6 of GalNAc (CSC), C-2 of GlcA and C-6 of GalNAc (CSD), or C-4 and C-6 of GalNAc (CSE)[3]. CS GAGs average approximately 21.5 kDa in molecular weight and are linked to core proteins. Sulfated CS binds the secreted growth factor Nodal[31]. CSA binds opticin (OPT)[32] and Indian Hedgehog[33], but not Pleiotrophin[34], FGFs3, 5, 6, 8, or 22[35], or BMP4[36] that bind only CS chains with 2 sulfates per disaccharide.

Non-sulfated anionic HA, first discovered in ocular vitreous humor[37], is composed of repeating –[4GlcAβ1-3GlcNAcβ1]-disaccharide units, is synthesized on the plasma membrane with no

attachment to any core protein, and is very large, with molecular weights from 100-10,000 kDa. HA non-covalently binds several PGs (aggrecan[38], versican[39], neurocan[40], and brevican[41]), link proteins[42], TNF-stimulated Gene 6 (TSG-6)[43], and the receptor CD44[44] through a link module known as the PG tandem repeat (PTR) module[45]. Other HA-binding proteins include fibronectin[46], Receptor for HA Mediated Mobility (RHAMM)[47,48], and intracellular adhesion molecule-1 (ICAM-1)[49]. There is increasing evidence that HA occurs intracellularly[50,51], as well as extracellularly.

In developing chick embryos, neurorepellant ECM component Semaphorin 3A (SEMA3A), secreted by the lens, strongly influences when neural crest-derived corneal peripheral nerve axons invade the corneal anterior stroma and extend and branch through the anterior stroma and corneal epithelium[52]. Corneal nerve growth cone penetration occurs, even though anterior stromal cells and corneal epithelial cells express SLIT2, a strong negative regulator of nerve growth, throughout chick embryonic development[53,54]. It has been suggested that, in the posterior E9 cornea, ECM-accumulated highly sulfated KS binds and thereby blocks the diffusion of lens SEMA3A, thus allowing anterior stromal penetration of corneal nerve growth cones to begin on E9, and that corneal nerves extend into the anterior stroma and eventually into the corneal epithelium to avoid increasing ECM accumulation of highly sulfated KS from posterior to anterior in the developing corneal stroma[53].

To test this hypothesis and identify other proteins that may interact with corneal GAGs, bovine corneal KS, sturgeon notochord CSA, and HA were biotinylated and used to screen an Invitrogen proteomics array of over 8000 intracellular and extracellular Version 4 (v4) proteins and a

separate custom array of 85 extracellular epitopes of neuroregulator receptors, ligands, and growth factors. Biotinylated corneal KS core protein mimecan (OGN) was also used to screen the v4 array. The least prevalent corneal KS core protein by % weight, it may play a major role in some functions, depending on its localization, and nothing is currently known about proteins it may bind. Corneal KS, sturgeon notochord CSA, and HA bound many of these proteins selectively, suggesting that KS, CSA, and HA could alter the availability or conformation of many proteins that may influence corneal keratocyte and nerve growth cone behavior.

Experimental Procedures:

Materials: Bovine corneal KS and sturgeon notochord CSA were purchased from Northstar BioProducts of Associates of Cape Cod, Inc. (ACC) (formerly Seikagaku America) (East Falmouth, MA). Biotinylated HA (bHA), *N*-Ethyl-*N*′-(3-dimethylaminopropyl)-carbodiimide (EDC), and biotin-X-hydrazide were purchased from Sigma-Aldrich (St. Louis, MO). BupH™ MES buffered saline packs and the biotin quantitation assay contained in the EZ-Link Sulfo-NHS-LC-Biotinylation Kit [product # 21435] were purchased from Thermo Scientific Pierce Protein Research Products (Rockford, IL). Amicon Ultra centrifugal filter (regenerated cellulose 3,000 MWCO) was purchased from Millipore-Biomanufacturing and Life Research Products, (Billerica, MA). Protoarray Version 4 proteins, Alexa-Flor 647-labeled goat anti-rat IgG, V5-his-tagged calmodulin kinase 1, and Alexa-Flor 647-labeled anti-V5 antibody were supplied by Invitrogen Corporation (Carlsbad, CA) as part of their protoarray service. All extracellular epitopes of nerve-related proteins listed in Table 1, mimecan protein, and rat anti-mouse mimecan antibody were purchased from R & D Systems (Minneapolis, MN). Surface Plasmon

Resonance (SPR) analysis was conducted on a BIAcore 3000, and the data were analyzed using BIAevaluation software 4.1 purchased from GE Healthcare, Biacore Life Sciences Division (Piscataway, NJ). Strepavidin (SA) coated Chips, Biotin CAPture Kits, and HEPES buffer with surfactant P20 (HBS-P) (10 mM HEPES, pH 7.4, 150 mM NaCl, 0.005% (v/v) Surfactant P20) running buffer were also purchased from GE/Biacore.

Preparation of Biotinylated KS: Seikagaku America purified KS by chromatography and chondroitinase ABC treatment, leaving a residual core peptide at the reducing terminus of KS chains. The average molecular weight of the purified KS was approximately 15 kDa. Attachment of biotin to free carboxy groups in the residual core peptide was carried out using the EDC protocol[55,56]. KS (1 mg) was dissolved in 0.5 ml 0.1 M MES [(2-N-morpholino) ethanesulfonic acid] (pH 4.5) containing 2 mg/ml biotin-LC-hydrazide and 20 mg/mL EDC. The mixture was rotated end-over-end at room temperature for 24 hours. Using an Amicon Ultra centrifugal filter (regenerated cellulose 3,000 MWCO), biotinylated KS (bKS) molecules were extensively washed with deionized H_20 to remove salt and free biotin, and then lyophilized. The yield of bKS was 0.8 mg. The (2-(4´-Hydroxyazobenzene) Benzoic Acid (HABA) assay was used for measuring the level of biotin incorporation, following the protocol described in the EZ-Link Sulfo-NHS-LC-Biotinylation Kit [Product # 21435]. Briefly, a calibration curve was obtained by adding biotin to 500 µL avidin-HABA reagent and measuring the decrease in absorbance at 500 nm. The biotin content of bKS was estimated by mixing 50 µL of the sample and 450 µL of the avidin-HABA reagent and comparing the absorbance at 500 nm with the standard. A biotinylation ratio of 1.43 moles biotin per mole KS was obtained, suggesting that

1-2 molecules of biotin were attached to each KS chain. Since there are no free carboxyl groups in the KS disaccharide, no biotin molecules were attached along the sides of the KS chain.

Preparation of Biotinylated CSA: Sturgeon notochord CSA was highly purified by chromatography by Seikagaku America. The average molecular weight of CSA was approximately 16 kDa. Purified CSA was labeled by EZ-link Biotin-LC-Hydrazide, and biotin was attached to carboxyl groups of uronic acid residues along the CSA GAG chain using the EDC protocol[55,56] as described above, beginning with 2 mg CSA dissolved in 1 ml 0.1 M MES (pH 4.5) containing 2 mg/mL biotin-LC-hydrazide and 20 mg/ml EDC. The yield of the biotinylated CSA (bCSA) was 1.7 mg. Using the HABA assay described above, a biotinylation ratio of 2.78 moles biotin per mole CSA was determined, which is equivalent to 7.6 residues of biotin for every 100 disaccharide residues.

Biotinylated HA: Biotinylated HA (bHA) was purchased directly from Sigma. Based on the certificate of analysis, the molecular weight of HA was 850 kDa. Biotin was attached by the manufacturer to carboxyl groups of glucuronic acid along the HA GAG chain, resulting in a degree of substitution of 6 mol %, which is equivalent to 6 residues of biotin for every 100 disaccharide residues.

GAG-Protoarrays: The Invitrogen Corporation Protoarray Version 4 is comprised of 8268 human proteins, most of which are produced in baculovirus expression systems as N-terminal glutathione S-transferase fusion proteins, and purified using glutathione S sepharose under non-denaturing conditions. These proteins, therefore, do not carry any of the post-translational

modifications, such as glycosylation side chains, that they may carry when synthesized in their normal human cell environment. All proteins were dissolved in printing buffer (PB) (50mM HEPES, 200mM NaCl, 0.08% Triton X-100, 25% glycerol, 20mM reduced glutathione, pH 7.5) at ~50 ng/ul. and spotted on nitrocellulose-coated glass slides. Protein purification and array printing were done at ~6 degrees C. A searchable list of these proteins may be viewed at: http://hdl.handle.net/2097/1716, including the amino acid sequence of the protein version spotted at each site, an estimate of the amount of protein in each spot for all GST-tagged proteins based on assay with an anti-GST antibody, and an Invitrogen account number or uIOH number for each protein that can be used at Invitrogen's website to find additional information about that protein. In order to assess reproducibility of protein binding for a test ligand within a single v4 assay run: (1) all proteins were spotted in duplicate at each location; (2) some v4 proteins were spotted at several different locations, either as slight variants containing small amino acid variations of other v4 proteins or as larger variants containing only partial sequences of the full-length protein whose name they bear in the searchable list (see below); (3) some kinases, recognized by a uIOH number starting with P or PV, have His tags rather than GST tags, and generally adhered to the nitrocellulose-coated glass slides at higher concentrations than GST tagged proteins. In conjunction with the KS v4 studies, a custom plate containing SEMA3A-Fc, spotted in dulicate in a four-step concentration gradient (5 ng/uL, 10 ng/uL, 20 ng/uL, and 40 ng/uL), was also prepared.

Printed plates were washed with PB, and then blocked with SMI buffer (50 mM Tris pH7.5, 5 mM Mg_2SO_4, 0.1% Tween-20, 1% BSA, with the 1% BSA acting as the blocking agent). They were then exposed to 1.5 ng/μL, 15 ng/μL, or 150 ng/μL of biotinylated test GAG suspended in

SMI buffer for 90 minutes at 4^{o}C. The arrays were washed 3 times, 5 minutes per wash, with 5 mL SMI buffer at 4^{o}C. Parallel negative (buffer alone) and positive (100 nM Alexa Flour 647-conjugated staurosporine, known to bind one of the proteins in the protoarray) control arrays were run simultaneously. Arrays were exposed to 1 μg/mL Alexa Fluor 647-conjugated strepavidin in SMI for 30 minutes at 4^{o}C. They were washed 3 times, 5 minutes per wash, in 5 mL SMI buffer at 4^{o}C, then quickly rinsed in water before drying and scanning.with an Axon 4000B fluorescent scanner (Molecular Devices). Data were acquired with GenePix Pro 6.0 software (Molecular Devises). The data were analyzed using Invitrogen ProtoArray Prospector software.

Four criteria were used to define a significant interaction between a v4 protein and bGAGs: [1] A Z-score, or normalized fluorescent signal, greater than 3.0 standard deviations above the mean human protein signal for non-reactive proteins in the test array, and a Z score less than 1.0 in the negative control assay. [2] A Z-Factor greater than 0.5, meaning that the signal was at least 2-fold greater than the negative control. [3] A Cl P-Value less than 0.05, where the Cl P-Value assigns a probability that the signal is derived from the distribution of signals arising from a set of defined negative controls. [4] A replicate spot CV less than 50%, where CV is the coefficient of variation for the assay from duplicate spots, determined by dividing the standard deviation of the spot signals for all of the spots by their mean spot intensity. A Z-score greater than 3 required a signal of ~15,600 RFU (relative fluorescent unit) or greater to be classified as a positive binding protein for KS, and a signal of ~13,000 RFU or greater to be classified as a positive binding protein for CSA. For HA, there were only two proteins that met these stringent threshold criteria, and thus a Z value greater than 1 was used to identify additional potential hits.

The custom SEMA3A-Fc plate, probed with bKS at the same time as the KS-v4 protoarray, was scored based on the presence of signal that was significantly higher than the signal seen when the custom array was probed with detection reagent alone (result included at the bottom of Table 2).

To further investigate binding of corneal stromal GAGs to ECM nerve-related molecules, we purchased selected extracellular epitopes of growth factors, nerve growth cone guidance ligands, and their receptors from R & D Systems, and asked Invitrogen to create a custom nerve-related protein array and assay binding of bKS, bCSA, and bHA to these proteins using their standard protocol. The protein epitopes used in this custom array are shown in Table 1. Each protein was spotted in duplicate from solutions of 10 ng/μL, 25 ng/μL, or 50 ng/μL in PB and bGAGs were used at 1.5 ng/μL, 15 ng/μL, or 150 ng/μL in SMI buffer. Proteins were scored as GAG binders if the difference between the RFU value measured on the negative control assay (buffer only) and the assay probed with the bGAG was greater than 2,000 RFU for any concentration of the probe GAG.

Mimecan Protoarray: The KS core protein mimecan was used by Invitrogen to probe its v4 protoarray, following the same format as described for GAG protoarrays, except that the test ligand was purified mouse mimecan, tested at 5 ng/μL and 50 ng/μL. Following incubation of the protoarray slides with mimecan, the slides were washed, incubated with rat anti-mouse mimecan, and then with Alexa-Flor 647-labeled goat anti-rat IgG. For the mimecan protoarray, the negative control was buffer alone, and the positive control was V5-his tagged yeast calmodulin kinase 1, developed with Alexa-Flor 647-labeled anti-V5 antibody. The reaction of

calmodulin kinase 1 with calmodulin protein in the v4 protoarray served as an indicator that the assay functioned properly. Data were acquired with GenePix Pro 6.0 software (Molecular Devises), and analyzed using Invitrogen ProtoArray Prospector software as described above. The criteria for a positive reaction between mimecan and a v4 protein were as described for the v4-bGAG assays.

Surface Plasmon Resonance: SA sensor chips were conditioned with 3 consecutive 1 minute injections of 1 M NaCl in 50 mM NaOH before ligand was immobilized. Biotinylated-KS was dissolved in 0.01 M HEPES pH 7.4, 0.15 N NaCl, 0.005% (v/v) Surfactant P20 (HSB-P) buffer at 0.01 mg/mL and immobilized on Flow cell (Fc) lanes 2-4 of an SA chip, using an inject time of 1 minute at a flow rate of 10 μL/min. A control of biotin alone was then immobilized on Fc lane 1 of each SA chip using a saturated solution of biotin in HSB-P buffer under the same protocol as above. The 4 lanes of the chip were then washed with HSB-P buffer according to Biacore protocol. Successful immobilization of biotinylated-KS was confirmed by a 290 to 300 RU increase [RU=resonance units, where one RU is equivalent to one picogram of protein per square millimeter on the sensor surface] in the appropriate sensor chip lane. RU increase for the biotin lane was less than 50 RU. All data were blanked against the biotin control reference Fc (Fc1), and double-referenced against an HBS-P buffer injection (SLIT2 at 0 nM). Protein samples were diluted in HSB-P. Protein solutions were passed over the biotin-KS coated sensor surface using the KINJECT mode at a flow rate of 20 μL/min with a total injection volume of 100 μL, which flowed over chip lanes sequentially from 1 to 4. After each run of a given protein concentration, dissociation was conducted in HSB-P buffer for 600 seconds, and regeneration of the sensor surface was conducted in 1M NaCl in 50 mM NaOH. The response was monitored as

a function of time (sensorgram) at 25^{o}C, using automated in-line reference subtraction to subtract biotin control ligand binding in Fc1 from biotin-KS ligand binding in Fc2, 3, and 4**.** The kinetic parameters k_a and k_d (association and dissociation rate constants, respectively) were analyzed simultaneously using Global Fit. BIAevaluation software Version 3.1 (BIAcore) simultaneously fitted the sensorgrams obtained at different concentrations of ligand, fixing each kinetic parameter to a single value for each set of experimental data. An apparent equilibrium dissociation constant (K_D) was calculated as the ratio k_d/k_a with the maximum capacity (R_{max}) of the surface floated during the fitting procedure.

Results:

KS, CSA, and HA bind human cellular proteins: Bovine corneal KS binding to a very wide variety of proteins was assessed by Invitrogen using their Version 4 (v4) Protoarray, with over 8000 human proteins or protein variations. A complete and searchable list of all v4 proteins, including an Invitrogen identification number, their location on v4 protoarray plates, an estimation of their concentration if they are GST-tagged proteins, and their exact amino acid sequence may be viewed at website (http://hdl.handle.net/2097/1716). When screened at 150 ng/μL (10μM), KS gave positive binding responses with 217 v4 proteins. With the exception of ABL1 homologue 1 variant a (see below), each protein that KS bound was listed only once in Table 2, at the level of its highest binding, even when alternative forms or amounts of the protein, present in the different locations on the protoarray slides, also interacted with KS. An expanded version of Table 2, showing all proteins at all locations on the v4 protoarray slides that reacted with KS can be viewed at http://hdl.handle.net/2097/1716. Extracellular SEMA3A linked to IgG_1 (see below), obtained from R & D Systems, also was included in this analysis, and

the response of 150 ng/μL bKS to 40 ng/uL SEMA3A-Fc is listed at the end of Table 2. Reproducibility of the KS-v4 protein binding results is supported in several ways. (1) The coefficient of variability of bKS binding to duplicate spots of a given protein at any one location in the v4 protoarray plates was never more than 12% for any positive KS-binding protein (see expanded Table 2 at http://hdl.handle.net/2097/1716). (2) Binding of bKS to ABL1 homologue 1 variant a, occurred at all 5 duplicate locations of ABL1 homologue 1 variant a in the v4 protoarray in which the variation between the ABL1 homologue 1 variant a's was only 1 amino acid, with very similar binding strengths of 43459, 38005, 36821, 35400, and 35199 (Table 2). In contrast, bKS did not bind severely truncated versions of ABL1 homologue 1 variant a spotted at two other locations (see locations 2178 and 2878 in the total v4 proteins list at http://hdl.handle.net/2097/1716). (3) 150 ng/μL bKS bound SEMA3A-Fc plated at 40ng/ μL in the first small custom protoarray shown at the end of Table 2 (5913 RFU) at a level very similar to its binding to SEMA3A-Fc plated at 50ng/μL in the second larger custom protoarray shown in Table 5 (8203 RFU).

Nine of the 217 respondents were still positive when the screening was conducted at 15 ng/μL KS (ABL1, TBK1, PLK1, AXL1, NUAK1, CHUK, CCNT1, KCNAB2, and RPS6KA1), whereas only KCNAB2 was positive when the screening was conducted at 1.5 ng/μL KS. Of proteins that bound 150 ng/μL KS, 75 were protein kinases, comprising several families: (a) 10 cytoplasmic tyrosine kinases: ABL2, ABL1, BMX, BTK, PTK2B, SRC, FES, HCK, YES, and LYN; (b) 15 cytoplasmic domains of receptor tyrosine kinases: EPHA2, EPHA3, EPHA8, Ntrk1, Ntrk2, Ntrk3, wt KIT, 2 KIT point mutations, CSF1R, FGFR1, KDR, a FLT3 point mutation, ERBB2, and AXL; (c) 4 MAP kinase family members: MAP2K2, MAP2K6, a MAP2K6 point

mutation, and MAP3K10; (d) 4 NIMA-related kinases: NEK1, NEK2, NEK3, and NEK4; (e) Casein kinase: epsilon 1, gamma 2, and gamma 3; (f) Aurora kinases: AURKA and AURKB; (g) Death-associated protein kinases: DAPK2, DAPK3; (h) Ribosomal protein S6 kinases: RPS6KB2, RPS6KA1, RPS6KA2, and RPS6KA4; (i) Testis-specific serine kinases: TSSK1B and TSSK2; (j) MAP/microtubule affinity regulating kinases: MARK4 and MARK2; and (k) STE20-related kinases: PAK1, STK24, and STK25. In addition there were 13 membrane or secreted proteins that bound to 150 ng/μL KS: COL23A1, KCNAB2, ITGA6, CACNB1, EBAG9, SIRPG, PCDHGC3, SCYE1, F11R, CAPRIN1, ADD2, SYTL2, and BAIAP2. KS also bound 18 proteins involved in actin or microtubule binding or regulation: ABLIM1, CTNNA1, EPB39, LIMCH1, PAK4, ADD2, MAP2, AURKA, AURKB, DMN2, TPPP, MARK2, MARK4, MAPRE1, KIF2C, KIF3B, CTNNA1, and ACTR1B; and 20 proteins known or thought to be involved in nervous tissue function: Ntrk1, Ntrk2, Ntrk3, EPHA2, EPHA3, EPHA8, CAPRIN, BAIAP2, MAP2K10, SYTL2, DCX, HOMER2, TPPP, GSK3B, KCNAB2, MAP2, MARK4, PQBP1, ACTR1B, and extracellular SEMA3A. For transmembrane tyrosine kinase-containing receptor proteins, Invitrogen expressed and plated only the intracellular domain in their v4 protoarray.

In comparison, sturgeon notochord CSA bound only 23 v4 proteins when the screening was conducted at 150 ng/mL, listed in Table 3. Of these, 7 (CSNK1A1, CHUK, PAK1, RPS6KA5, FLT1, MAP4K4, and GADD45GIP1) displayed their highest binding at a bCSA screening concentration of 15 ng/μL, while only 3 (PLK1, HADH, NUDT16L1) were still positive when the screening was done at 1.5 ng/μL. Of the CSA-binding proteins, 10 were kinases: 2 independent preparations of PLK1, CHUK, PAK1, RPS6KA5, FLT1, MAP4K4, CSNK1D, and

PAK4; 2 were nuclear proteins identified with the cell cycle or DNA or RNA binding: NUDT21 and GADD45GIP1; and 2 were cell surface or scaffold proteins: ITGA6 and HOMER2. Again, reproducibility of bCSA binding in this proteomics protocol is supported in several ways. (1) The coefficient of variability between adjacent duplicate protein spots never exceeded 16% (data not shown). (2) PLK1 was spotted in 4 different duplicate locations in the v4 protoarray. One duplicate PLK1 version at one location was the highest binder of bCSA (64679RFU) (Table 3), and had a His-tag instead of the usual GST tag on most v4 proteins, which caused it to be printed at a higher concentration than GST-tagged proteins. A second PLK1 duplicate spot location was the lowest reported binder of bCSA (19806RFU) (Table 3), and was plated at a lower concentration than was retained at the highest binding location. PLK1s plated at a third and a fourth location were plated at concentrations $1/4^{th}$ that of the concentration at the second location, the version at the 4^{th} location was severely truncated, and neither location gave a positive signal for bCSA binding. These results demonstrate a concentration dependency for CSA-protein binding.

In contrast, HA bound only 6 of the over 8000 Invitrogen v4 proteins, listed in Table 4. Of these 6 proteins, 3 (KRTAP13-1, IRS1, and HADH) achieved their highest binding at an HA screening concentration of 150 ng/μL, 1 (LGALS8) showed its highest binding at an HA screening concentration of 15 ng/μL, and 2 (GFAP and CABP4) displayed their highest binding at an HA screening concentration of 1.5 ng/μL. Overall, the signal intensity for all 3 bHA screenings was low compared to the signal intensities for bKS and bCSA screenings, with only KRTAP13-1 generating a signal intensity above the lowest positive v4 intensities obtained with bKS and

bCSA. Again, the coefficient of variability between adjacent duplicate spots was never higher than 16% (data not shown), suggesting good binding reproducibility for bHA. In addition, although only 1 of the 6 v4 proteins bHA bound was present more than once in the v4 protoarray, a complete version of galectin 8 [LGALS8] and a variant version lacking an internal segment of the protein and plated at about 1/10th the concentration of the complete version, bHA bound the more concentrated complete version at a level significantly above background noise, but did not bind the much less concentrated variant lacking the internal segment. While these results could reflect either the avidity of HA for LGALS8 or the ability of HA to discriminate between full length and internally truncated LGALS8, they suggest that the protoarray protocol used in our experiments allowed bHA to bind protein spots discriminately.

KS, CSA, and HA bind extracellular epitopes of nerve-related proteins: The anterior cornea is one of the most highly innervated tissues on the surface of the human body[57]. Because KS, CSA, and HA are present in very high concentrations in the corneal ECM, we asked whether these GAGs bind some of the neuroregulatory molecules or epitopes of membrane-bound neuroregulatory molecules whose mRNAs are known to be expressed in the developing cornea[53]. Because of our previous localization of SLIT2 mRNA in the anterior cornea and the high amino acid sequence homology between SLIT orthologues[58], we included SLIT3 in our custom array because it was the only SLIT orthologue R & D Systems had available at the time.

Bovine corneal bKS bound 44 of the 85 nerve-related proteins or protein epitopes for the nerve-related custom protoarray analysis, listed in Table 5. In addition to the high similarity of bKS binding to SEMA3A-FC shown in both the first and the second custom array experiments (see

above), reproducibility of bKS-nerve-related-protein-binding is supported by its concentration dependancy. For the nerve-related protein custom arrays, all proteins were plated in duplicate spots at 3 or 4 separate locations at different concentrations, and screened with 3 different GAG concentrations. For many KS interactant proteins, there was a concentration-dependent increase in RFU signal with increasing signals being observed both with higher KS concentrations and at spots corresponding to higher concentrations of protein on the arrays (data not shown).
In agreement with the results of preliminary tests (see Methods), in 20 of the 29 sets of IgG_1-tagged/cleaved target protein epitopes, bKS bound the IgG_1-tagged version of the protein, but not the IgG_1-cleaved version. In 2 additional cases (SEMA3F and SEMA6A), KS bound the IgG_1-tagged version better than the IgG_1-cleaved version; in 1 case (ERBB4) KS bound the IgG_1-cleaved version better than the IgG_1-tagged version, and in 6 cases KS bound neither version (Ntrk1, EPHA2, EPHA5, EPHB2, EPHB6, and NRP2).

Of the 85 nerve-related epitopes in the protoarray, bKS bound most strongly the neuroregulatory ligand SLIT3; KS also bound the extracellular epitopes of SLIT receptors ROBO1 and ROBO2. The second and third most strongly bound epitopes were “deleted in colorectal carcinoma” (DCC), a netrin receptor, and ERBB4, a neuregulin receptor. KS bound all of the neuroguidance SEMA epitopes in the protoarray, but did not bind either of the SEMA receptor epitopes, neuropilin 1 or neuropilin 2 (NRP1 or NRP2). There were no NRP co-receptor plexin epitopes available for the nerve-related protoarray. In the EFN/EPH neuroguidance family, KS bound the extracellular epitopes of all of the EFN ligand epitopes in the protoarray, but only 9 out of 13 EPH receptor epitopes in the protoarray. In the NTN/DCC/UNC5H family, KS bound all of the NTN soluble ligand epitopes in the array, the one DCC receptor epitope in the array, and 1 of the

4 “uncoordinated 5H” (UNC5H) negative NTN receptor epitopes in the array. In the neuroattractant NT/Ntrk family, KS did not bind the soluble NT-3 neuroattractant ligand, but did bind the NT3-specific Ntrk3 receptor epitope and the less NT isoform-specific NGFR receptor. KS did not bind the other two NT receptors, Ntrk1 and Ntrk2. In the Schwann cell regulating NRG/ERBB family, KS bound both the soluble NRG1 SMDF Schwann cell attractant/stimulatory ligand, and the two SMDF ERBB receptor epitopes that were in the protoarray. Of the other soluble growth factors in the protoarray, KS bound PDGF, but did not bind EGF, acidic or basic FGF, or TGFβ1. Finally, KS did not bind either of the assembled integrin epitopes in the protoarray, Integrin alpha V beta 3 (αVβ3) or Integrin alpha 3 beta 1 (α3β1).

In comparison, sturgeon notochord CSA bound only 9 of the 85 nerve-related proteins or protein epitopes in the nerve-related protoarray, listed in Table 6. Secreted neuroguidance ligand NTN4 and one of its UNC5H negative receptor epitopes were the strongest CSA binders, whereas the DCC positive receptor epitope bound less strongly, and the other NTN and UNC5H isoforms in the protoarray were not bound by CSA. Two neuroregulatory SEMA isoform epitope ligands were slightly bound, along with 2 EFN ligands, 1 EFN receptor EPH epitope isoform, and 1 SLIT neuroguidance receptor ROBO epitope isoform. Of the 29 epitopes that were present in the protoarray in both the IgG_1-tagged and IgG_1-cleaved forms, CSA bound 5, and in each case it bound the tagged version, but not the cleaved version. Binding strengths for nerve-related CSA binders were significantly lower than were binding strengths for KS binders (compare Table 6 to Table 5).

bHA did not bind any proteins in the nerve-related extracellular epitope protoarray.

KS core protein Mimecan interactions with Invitrogen V4 proteins. The KS core protein mimecan (OGN) bound 15 of the 8000+ proteins in the v4 array, listed in Table 7. Of these 15 proteins, mimecan bound SLAIN2, a ubiquitously expressed beta-tubulin-like protein of unknown function that is widely conserved in vertebrates[59], with a higher signal than any signal generated by bKS, bCSA, or bHA binding to any protein. The next highest binder, UBXD3, generated 1/5th the signal intensity, and the other 13 binders gave signal intensities below 1/5th the mimecan-SLAIN2 intensity. Mimecan binders included 2 members of the casein kinase 1 family, delta and epsilon, 2 different potassium channel proteins, KCNAB1 and KCNAB2, and 3 kinases that have roles in microtubule formation or stabilization, MARK2, AURKA, and PLK1.

Kinetic studies of KS interaction with SLIT2 as determined by Surface Plasmon Resonance. Our protoarray study revealed SLIT3 to be one of the most avid binders to KS. After the nerve-related protoarray had been completed, R& D Systems made SLIT2 available. Because SLIT2 mRNA is expressed in the anterior cornea[54] and has been shown to influence nerve growth cone migration differently depending on whether it is bound by ECM molecules[60,61], we characterized the interaction of KS with SLIT2 in more detail, performing Surface Plasmon Responance (SPR), with bKS immobilized on strepavidin-coated sensor chips. The kinetic analyses were performed by injecting SLIT2 at various concentrations over immobilized KS. As revealed by a typical sensorgram shown in Figure 1, binding of SLIT2 to KS was concentration-dependent. For the analyses shown in Figure 1, the SLIT2 injection volume was 50 μL. Kinetic analyses for each SLIT2 concentration were performed in triplicate. As shown in Figure 2, SLIT2 binds to

KS in a saturable manner, as evidenced by the logarithmic trend line. Kinetic data were fitted to a 1:1 Langmuir binding model, allowing the calculation of the k_a (kinetic association rate constant), the k_d (kinetic dissociation rate constant), and the K_D (apparent equilibrium dissociation constant), shown in Table 8. The K_D for SLIT2 binding to KS was 28 nM, suggesting that KS binds SLIT2 with relatively high affinity.

By protoarray analysis, KS bound SEMA3A much less strongly than SLIT3, but binding was still significantly above background (Table 2 and Table 5). Repeated attempts to detect SEMA3A binding to immobilized KS using SPR were unsuccessful using SEMA3A concentrations as high as 2 μM, or 250 ng/μL.

Discussion:

In both Invitrogen's v4 protoarray and a custom extracellular nerve-related protoarray, corneal KS bound the greatest number of proteins. In contrast, sturgeon notochord CSA bound significantly fewer v4 proteins and extracellular nerve-related proteins than KS. Non-sulfated HA bound the fewest v4 proteins in comparison to corneal KS and sturgeon notochord CSA, and no extracellular nerve-related proteins at all. Mimecan, included in this study because it is the KS core protein about which the least protein-binding information is known, bound slightly more v4 proteins than sturgeon notochord CSA, and was not tested with our custom extracellular nerve-related protein array. However, binding strengths of 9 of the 23 sturgeon notochord CSA-binding candidates were higher than the binding strength of the strongest corneal KS-binding candidate. In contrast, binding strengths of 5 of the 6 HA-binders were lower than the strengths of any positive corneal KS- or highly sulfated CSA-binding proteins. Both corneal KS and

sturgeon notochord CSA bound preferentially with the biologically active (IgG_1-tagged) form of almost all extracellular nerve-related epitope pairs, suggesting that the GAG-protein interactions observed in this study have potential *in vivo* relevance. Although generally regarded as extracellular, KS[24,62-66] and HA[50,51] have also been detected intracellularly. These GAG-protein binding profiles demonstrate that GAGs found in the corneal stroma may interact with many proteins, both intracellularly and extracellularly, and thus could influence the availability and/or the configuration of these proteins for subsequent interaction with their target cellular ligands/receptors.

Our study is the first to examine binding of corneal KS, sturgeon notochord CSA, or non-sulfated HA to a wide variety of cellular and ECM proteins using high through-put protoarray techniques with the proteins immobilized on a fixed surface and the GAGs free in solution. Other protoarray studies examining GAG-protein interactions have immobilized naturally occurring and synthetic GAGs on a fixed surface and probed them with solutions containing a limited number of known proteins[67, 68]. That the protoarray format can reveal new protein-GAG interactions is substantiated by the fact that the Wang study[68] revealed dermatan sulfate GAG binding to an antibody not previously thought to bind dermatan sulfate GAG. In our study the protoarray format first revealed KS binding to a SLIT family member, which was then further defined for KS binding to SLIT2 by SPR studies. It is not clear from our and other comparative protein-GAG interaction studies whether it is better to attach the GAG or the protein to the fixed matrix, and what is optimal may differ for different GAGs and different proteins. Attaching some GAGs[69] and proteins[70] to a matrix has been found to impose structural constraints on them that have diminished their binding to some proteins. Also, some GAGs[67,71] and some proteins

may attach better to a given matrix than others. In our study HA in solution did not bind known HA-binders aggrecan, Link protein, and fibronectin affixed to a matrix, but it has been shown to bind link module when HA is the fixed moiety[45,72]. In our study KS in solution bound SEMA3A in the protoarray format where SEM3A was the fixed moiety, but not in the SPR format where KS was the fixed moiety.

Whereas there are several indicators of reproducibility for the protein binders for KS, CSA, and HA detected in our protoarray protocol, our protocol failed to detect binding of some of these GAGs to proteins they have been reported to bind in other studies, such that these known GAG binders did not serve as positive controls in our protoarray study. The most probable reason that the v4 versions of aggrecan, Link protein, or fibronectin did not serve as positive controls for HA binding in our proteomics study is that the v4 versions of these proteins are produced in insect cells and are therefore not glycosylated in the ways that these molecules are when produced under their usual human cell biosynthetic conditions. Deglycosylated aggrecan can not bind HA[73], and it is likely that the same is true for nonglycosylated Link protein. In addition, fibronectin binding of HA requires that the fibronectin be both glycosylated and aggregated, and nonaggregated firbronectin bound to an affinity column does not bind HA[74]. In the same vein, although KS had been shown to bind IGFBP2 prior to this proteomics study, IGFBP2 could not serve as a positive control for KS binding in our proteomics screening format because IGFBP2 binds GAGs only if IGF-I or IGF-II are present[75]. These considerations suggest that the proteins identified as GAG binders in our protoarray format bind those GAGs without being post-translationally glycosylated or the participation of additional cofactors.

In many GAG-protein interaction studies, biotinylation is a common method for labeling either the proteins or the GAGs. In some protoarray studies, soluble protein ligands are labeled with biotin for detection after GAG binding[67,68]. Our study used immobilized proteins with solubilized bGAGs for detection. Other studies have also used bGAGs to study GAG interactions with immobilized proteins[71-72, 75-78]. However, biotinylation procedures can biotinylate different positions within a GAG[69], as occurred in our study with biotinylation of KS only at one end of its chain and biotinylation of CSA and HA all along their GAG backbones. In addition, biotinylation can have different efficiencies with different GAGs, again as it did in our study. These differences in biotinylation may have different effects on the functional properties of GAGs[69,71,79]. Similar position, efficiency, and steric hinderance effects may perturb the binding properties of proteins if they are the biotinylated moieties in GAG-protein binding studies. Also, many GAG-protein interaction studies using column chromatography or SPR protocols use the biotin of the bGAG to attach the GAG to the fixed substrate[32,69,80], as we did in our SPR experiments. This could magnify structural aberrations in a GAG to a greater or lesser extent depending on where the GAG is biotinylated. Thus, protoarray techniques can suggest false GAG-protein interactions, and proteins identified by protoarray studies as GAG-binding proteins should be considered "candidate" GAG-binders until additional techniques confirm the GAG-protein binding.

GAGs are defined by their primary disaccharide structure, and therefore KS, CS, and HA have the same primary structure from one species to another. However, the extent and positions of sulfation of GAG disaccharides can vary considerably for any one kind of GAG, both from species to species, and also from tissue to tissue within a given species. Bovine and human corneal KS chains have similar charge densities and chain lengths, and the 3 most prevalent

capping structures at the non-reducing termini are identical in relative proportions[81]. Therefore it is likely that human corneal KS chains would bind Invitrogen v4 human proteins in a manner very similar to that displayed by bovine corneal KS. In contrast, sturgeon notochord CSA is 100% sulfated[82] (every disaccharide is monosulfated at C-4 of GalNAc), which is a higher percentage of disaccharide sulfation than is found in most human[83] or bovine[82] corneal CSA. The extent and positions of sulfate groups within CS chains have been shown to significantly affect CS binding to protein targets[33,34,84], leading to the proposal of a "sulfation code"[85] for GAGs that governs their ability to interact with proteins. It is not known whether human corneal CSA chains may be asymmetrically sulfated, such that they have regions of high (100%) disaccharide sulfation contiguous with regions of low disaccharide sulfation. If they do, 100% sulfated regions (sulfation "hot spots") of such human corneal CSA would be expected to show protein-interactions similar to those seen with sturgeon notochord CSA, whereas the low sulfated regions might bind very different proteins. HA is never sulfated, so HA from any species or tissue should be equivalent in its binding properties with human proteins, as long as their average chain lengths are similar.

In our GAG protoarray studies, Invitrogen optimized conditions for KS binding in their protoarray protocol, and then used the same general conditions for CSA and HA binding. It is possible that under other binding conditions, highly (or asymmetrically) sulfated CSA, and/or HA might react with more candidate proteins. Alternatively, spotting complete post-translationally modified forms of proteins such as aggrecan, link protein, or fibronectin on microarray plates might also increase the number and kinds of proteins that bind GAGs in a

protoarray format. No mimecan binding proteins were known prior to our study, so it is difficult to assess whether the binding conditions used in this study were optimal for mimecan.

Because corneal KS, sturgeon notochord CSA, and HA are large linear polyanionic molecules, it is probable that electrostatic interactions are part of the mechanism involved in the protein-KS, -CSA, and -HA binding observed in our protoarray studies, as has been demonstrated in many heparin- and heparan sulfate-protein interactions[86]. Recent studies of reactions of yeast[87] and human[88,89] protein arrays with a range of biotinylated linear polyanionic macromolecules (actin, tubulin, heparin, heparan sulfate, and DNA) have defined a wide array of polyanionic binding proteins (PABPs), with sulfated GAGs binding the greatest number of different PABPs in each study. Additionally, lack of reduction in the number of PABPs bound by increasing binding solution salt concentrations suggests that there are also non-coulumbic (e.g. hydrophobic and hydrogen binding) molecular interactions involved in protein-GAG binding[88,89]. Moreover, reacting proteins did not need to be positively-charged overall, nor to have a specific GAG-binding "signature" sequence motif[18], but only needed to have some positive subdomain along their amino acid sequence to be capable of polyanionic binding[86-89]. The authors argue that many proteins contain subdomains of amino acids that are probably unfolded in solution[90], and that these disordered regions may allow them to interact with many different binding partners with varying degrees of strength or specificity by mechanisms such as electrostatic interaction that do not require tertiary structure complementarity. Similar considerations also apply to interactions of proteins like kinases with smaller anionic molecules such as single nucleotides[89]. In our study, 75 of the 217 KS-candidate v4 protein binders and 9 of the 23 CSA-candidate v4 protein binders were kinases. The catalytic domains of all kinases contain two invariant lysines

and an arginine, with the serine/threonine kinases containing an additional invariant lysine, and the tyrosine kinases containing additional histidine, arginine, and lysine residues[91], suggesting that kinase catalytic domains may have an overall basic charge that would allow them to interact electrostatically with polyanionic GAGs. Viewed more broadly, 28 of the top 50 KS-candidate binders and 11 of the 23 CSA-candidate binders could be classified as PABPs on the basis of their known binding to actin, microtubules, DNA, RNA, nucleotides, or nucleosides. HA's top protein interactants could also be viewed as potential PABPs. Keratin-associated protein 13-1, KRTAP13-1, contains one partial (-RPR-) basic amino acid-rich GAG-binding motif [18] in its short sequence[92]. Insulin receptor substrate 1, IRS1, possesses numerous basic amino acid-rich segments in its primary amino acid sequence and 2 ATP-binding sites[93,94].

The nature of the interactions between mimecan and its 15 candidate v4 protein binding partners remains unresolved. The revelation that mimecan binds SLAIN2, a beta-tubulin-like protein, and 3 kinases that regulate microtubule behavior suggests a possible role for mimecan in microtubule function in vivo. It is probable that the protein-binding behavior of mimecan core protein is altered when it is glycosylated with KS chains. Although all three corneal KS core proteins are small leucine-rich repeat proteins, mimecan is smaller than the other two proteins[4,5,6]. It would be interesting to know whether the protein binding properties of KS are affected differently when it is attached to different core proteins.

SLIT-1, -2, and -3 orthologs usually function as chemorepellants of migrating neuronal growth cones[95]. However, an N-terminal fragment of SLIT2, purified from rat brain, causes DRG sensory axons to elongate and branch[96]. Full-length neurorepellant SLIT2 can be transformed

into neuroattractant and bifurcation N-terminal SLIT2 by interaction with ECM components[61], including rat brain heparan sulfate proteoglycan Glypican-1(GPC1)[97]. Heparan sulfate *O*-sulfate groups are critical for GPC1-SLIT2 binding[98]. The mechanism of the proteolytic SLIT cleavage that results from GPC1-SLIT binding is not yet known. Our protoarray and SPR demonstrations that SLIT2 binds significantly to highly sulfated corneal KS suggests that polyanionic, highly *O*-sulfated ECM KSPG may function as a SLIT2-cleavage facilitator in the cornea, thus converting SLIT2 into its neuroattractant/neurobifurcating form in the area of the developing cornea where corneal nerves are extending and branching extensively[53,54]. This possible "chaperone" role for polyanionic KS in SLIT2 transformation indeed would mimic the role of polyanionic regions in other better-known chaperone-protein interactions[99-101]. In addition, under protoarray conditions, ECM neurorepellant SEMA3A was identified as a candidate KS binder. Perhaps association and dissociation constants for SEMA3A with KS could not be determined by SPR because of increased steric hinderance in KS function when it is the moiety attached to the fixed substrate. Our observations suggest that corneal KS may be very influential in regulation of corneal innervation during development.

References:

1. Gipson IK, Joyce NC, Zieske JD. 2004. The anatomy and cell biology of the human cornea, limbus, conjunctiva and Adnexa. In: Smolin and Thoft's The Cornea, Scientific Foundations and Clinical Practice. Fourth Edition. By Smolin G, Foster CS, Azar DT, Dohman CH. Lippincott, Williams, & Wilkins. 2004. pp 3-37.

2. Meyer K, Linker A, Davidson EA, Weissman B. The mucopolysaccharides of bovine cornea. *J Biol Chem.* 1953;205:611-616.

3. Davidson EA, Meyer KJ. Chondroitin, a new mucopolysaccharide. *J Biol Chem.* 1954;211:605-611.

4. Funderburgh JL, Funderburgh ML, Brown SJ, Vergnes JP, Hassell JR, Mann MM, Conrad GW. Sequence and structural implications of a bovine corneal keratan sulfate proteoglycan core protein. Protein 37B represents bovine lumican and proteins 37A and 25 are unique. *J Biol Chem.* 1993;268:11874–11880.

5. Funderburgh JL, Corpuz LM, Roth MR, Funderburgh ML, Tasheva ES, Conrad GW. Mimecan, the 25-kDa corneal keratan sulfate proteoglycan, is a product of the gene producing osteoglycin. *J Biol Chem*. 1997;272:28089-28095.

6. Corpuz LM, Funderburgh JL, Funderburgh ML, Bottomley GW, Prakash S. Conrad GW. Molecular cloning and tissue distribution of keratocan. Bovine corneal keratan sulfate proteoglycan 37A. *J Biol Chem.* 1996;271:9759–9753.

7. Li W, Vergnes JP, Cornuet PK, Hassell JR. cDNA clone to chick corneal chondroitin/dermatan sulfate proteoglycan reveals identity to decorin. *Arch Biochem Biophys.* 1992;296:190-197.

8. Bianco P, Fisher LW, Young MF, Termine JD, Robey PG. Expression and localization of the two small proteoglycans biglycan and decorin in developing human skeletal and non-skeletal tissues. *J Histochem Cytochem.* 1990;38:1549-1563.

9. Conrad G, Hamilton C, Haynes E. Differences in glycosaminoglycans synthesized by fibroblast-like cells from chick cornea, heart, and skin. *J Biol Chem.* 1977;252:6861-6870.

10. Trelstad RL, Hayashi K, Toole BP. Epithelial collagens and glycosaminoglycans in the embryonic cornea. Macromolecular order and morphogenesis in the basement membrane. *J Cell Biol.* 1974;62:815-830.

11. Fitzsimmons TD, Fagerholm P, Harfstrand A, Schenholm M. Hyaluronic acid in the rabbit cornea after excimer laser superficial keratectomy. *Invest. Ophthalmol. Vis. Sci.* 1992;33;3011-3016.

12. Groves ML, McKeon R, Werner E, Nagarsheth M, Meador W, English AW. Axon regeneration in peripheral nerves is enhanced by proteoglycan degradation. *Exp Neurol.* 2005;195:278-92.

13. Manton KJ, Leong DF, Cool SM, Nurcombe V. Disruption of heparan and chondroitin sulfate signaling enhances mesenchymal stem cell-derived osteogenic differentiation via bone morphogenetic protein signaling pathways. *Stem Cells.* 2007;25:2845-2854.

14. Miao HQ, Ishai-Michaeli R, Atzmon R, Peretz T, Vlodavsky I. Sulfate moieties in the subendothelial extracellular matrix are involved in basic fibroblast growth factor sequestration, dimerization, and stimulation of cell proliferation. *J Biol Chem.* 1996;271:4879-4886.

15. Fthenou E, Zafiropoulos A, Tsatsakis A, Stathopoulos A, Karamanos NK, Tzanakakis GN. Chondroitin sulfate A chains enhance platelet derived growth factor-mediated signalling in fibrosarcoma cells. *Int J Biochem Cell Biol*. 2006;38:2141-2150.

16. Fthenou E, Zafiropoulos A, Katonis P, Tsatsakis A, Karamanos NK, Tzanakakis GN. Chondroitin sulfate prevents platelet derived growth factor-mediated phosphorylation of PDGF-Rbeta in normal human fibroblasts severely impairing mitogenic responses. *J Cell Biochem*. 2008;103:1866-1876.

17. Aguiar CB, Lobão-Soares B, Alvarez-Silva M, Trentin AG. Glycosaminoglycans modulate C6 glioma cell adhesion to extracellular matrix components and alter cell proliferation and cell migration. *BMC Cell Biol.* 2005;6:31-39.

18. Cardin AD, Weintraub HJ. Molecular modeling of protein-glycosaminoglycan interactions. *Arteriosclerosis.* 1989;9:21-32.

19. Ruoslahti E, Engvall E. Complexing of fibronectin glycosaminoglycans and collagen. *Biochim Biophys Acta.* 1980;631:350-358.

20. Oldberg A, Ruoslahti E. Interactions between chondroitin sulfate proteoglycan, fibronectin, and collagen. *J Biol Chem.* 1982;257:4859-4863.

21. Funderburgh JL. Keratan sulfate: structure, biosynthesis, and function. *Glycobiology* 2000;10:951–958.

22. Aplin JD, Hey NA, Graham RA. Human endometrial MUC1 carries keratan sulfate: characteristic glycoforms in the luminal epithelium at receptivity. *Glycobiology* 1998;8:269–276.

23. Takahashi K, Stamenkovic I, Cutler M, Dasgupta A, Tanabe KK. Keratan sulfate modification of CD44 modulates adhesion to hyaluronate. *J Biol Chem.* 1996;271:9490–9496.

24. Akhtar S, Davies JR, Caterson B. Ultrastructural immunolocalization of alpha-elastin and keratan sulfate proteoglycan in normal and scoliotic lumbar disc. *Spine.* 2005;30:1762-1769.

25. Block JA, Inerot SE, Kimura JH, Heterogeneity of keratan sulfate substituted on human chondrocytic large proteoglycans. *J Biol Chem*. 1992;267:7245-52..

26. Funderburgh JL, Caterson B, Conrad GW. Keratan sulfate proteoglycan during embryonic development of the chicken cornea. *Dev Biol.* 1986;116:267–277.

27. Funderburgh JL, Funderburgh ML, Rodrigues MM, Krachmer JH, Conrad GW. Altered antigenicity of keratan sulfate proteoglycan in selected corneal diseases. *Invest. Ophthalmol. Vis. Sci.* 1990;31:419–428.

28. Vyas KA, Patel HV, Vyas AA, Wu W. Glycosaminoglycans bind to homologous cardiotoxins with different specificity. *Biochemistry.* 1998;37:4527-4534.

29. Russo VC, Bach LA, Fosang AJ, Baker NL, Werther GA. Insulin-like growth factor binding protein-2 binds to cell surface proteoglycans in the rat brain olfactory bulb. *Endocrinology.* 1997;138:4858-4867.

30. Carlson EC, Lin M, Liu CY, Kao WW, Perez VL, Pearlman E. Keratocan and lumican regulate neutrophil infiltration and corneal clarity in lipopolysaccharide-induced keratitis by direct interaction with CXCL1. *J Biol Chem.* 2007;282:35502-35509.

31. Oki S, Hashimoto R, Okui Y, Shen MM, Mekada E, Otani H, Saijoh Y, Hamada H. Sulfated glycosaminoglycans are necessary for Nodal signal transmission from the node to the left lateral plate in the mouse embryo. *Development.* 2007;134:3893-904.

32. Hindson VJ, Gallagher JT, Halfter W, Bishop PN. Opticin binds to heparan and chondroitin sulfate proteoglycans. *Invest Ophthalmol Vis Sci*. 2005;46:4417-4423.

33. Cortes M, Baria AT, Schwartz NB. Sulfation of chondroitin sulfate proteoglycans is necessary for proper Indian hedgehog signaling in the developing growth plate. *Development*. 2009;136:1697-1706.

34. Maeda N, Fukazawa N, Hata T. The binding of chondroitin sulfate to pleiotrophin/heparin-binding growth-associated molecule is regulated by chain length and oversulfated structures. *J Biol Chem.* 2006;281:4894-4902.

35. Asada M, Shinomiya M, Suzuki M, Honda E, Sugimoto R, Ikekita M, Imamura T. Glycosaminoglycan affinity of the complete fibroblast growth factor family. *Biochim Biophys Acta.* 2009;1790:40-48.

36. Miyazaki T, Miyauchi S, Tawada A, Anada T, Matsuzaka S, Suzuki O. Oversulfated chondroitin sulfate-E binds to BMP-4 and enhances osteoblast differentiation. *J Cell Physiol*. 2008;217:769-777.

37. Meyer K, Palmer JJ. The polysaccharide of the vitreous humor. *J Biol Chem*. 1934;107:629-634.

38. Hardingham TE, Muir H. The specific interaction of hyaluronic acid with cartilge proteoglycans. *Biochim Biophys Acta* 1972;279:401-405.

39. LeBaron RG, Zimmermann DR, Ruoslahti E. Hyaluronate binding properties of versican. *J Biol Chem.* 1992;267:10003-10010.

40. Rauch U, Karthikeyan L, Maurel P, Margolis RU, Margolis RK. Cloning and primary structure of neurocan, a developmentally regulated, aggregating chondroitin sulfate proteoglycan of brain. *J Biol Chem.* 1992;267:19536-19547.

41. Yamada H, Watanabe K, Shimonaka M, Yamaguchi Y. Molecular cloning of brevican, a novel brain proteoglycan of the aggrecan/versican family. *J Biol Chem*. 1994; 269:10119-10126.

42. Perides G, Lane WS, Andrews D, Dahl D, Bignami A. Isolation and partial characterization of a glial hyaluronate-binding protein. *J Biol Chem*. 1989;264:5981-5987.

43. Lee TH, Wisniewski H-G, Vilcek J. A novel secretory tumor necrosis factor-inducible protein (TSG-6) is a member of the family of hyaluronate binding proteins, closely related to the adhesion receptor CD44. *J Cell Biol.* 1992; 116:545–557.

44. Aruffo A, Stamenkovic I, Melnick M, Underhill CB, Seed B. CD44 is the principal cell surface receptor for hyaluronate. *Cell*. 1990;61:1303-1313.

45. Kohda D, Morton CJ, Parkar AA, Hatanaka H, Inagaki FM, Campbell ID, Day AJ. Solution structure of the link module: A hyaluronan-binding domain involved in extracellular matrix stability and cell migration. *Cell* 1996;86:767-775.

46. Yamada KM, Kennedy DW, Kimata K, Pratt RM. Characterization of fibronectin interactions with glycosminoglycans and identification of active proteoplytic fragments. *J Biol Chem.* 1980;255:6055-6063.

47. Sohr S, Engeland K. RHAMM is differentially expressed in the cell cycle and downregulated by the tumor suppressor p53. *Cell Cycle* 2008;7:3448–3460.

48. Day AJ, Prestwich GD. Hyaluronan-binding proteins: tying up the giant. *J Biol Chem*. 2002;277:4585-4588.

49. Gustafson S, Bjork T, Forsberg N, Lind T, Wikstrom T, Lidholt K. Accsssible hualuronan receptors identical to ICAM-1 in mouse mast-cell tumors. *Glycoconj J.* 1995;12:350-355.

50. Evanko SP, Wight TN. Intracellular localization of hyaluronan in proliferating cells. *J Histochem Cytochem.* 1999;47:1331-1342.

51. Collis L, Hall C, Lange L, Ziebell M, Prestwich R, Turley EA. Rapid hyaluronan uptake is associated with enhanced motility: implications for an intracellular mode of action. *FEBS Lett.* 1998;440:444-449.

52. Lwigale PY, Bronner-Fraser M. Lens-derived Semaphorin3A regulates sensory innervation of the cornea. *Dev Biol.* 2007;306:750-759.

53. Conrad AH, Strafuss JM, Wittman MD, Conway S, Conrad GW. Thyroxine increases the rate but does not alter the pattern of innervation during embryonic chick corneal development. *Invest. Ophthalmol. Vis. Sci.* 2008;49:139-153.

54. Conrad AH, Albrecht M, Pettie-Scott M, Conrad GW. Embryonic corneal Schwann cells express some Schwann cell marker mRNAs, but no mature Schwann cell marker proteins. *Invest. Ophthalmol. Vis. Sci.* 2009 50: 4173-4184.

55. Osmond RI, Kett WC, Skett SE, Coombe DR. Protein-heparin interactions measured by BIAcore 2000 are affected by the method of heparin immobilization. *Anal Biochem.* 2002;310:199-207.

56. Saito A, Munakata H. Detection of chondroitin sulfate-binding proteins on the membrane. *Electrophoresis.* 2004;25:2452-2460.

57. Müller LJ, Marfurt CF, Kruse F, Tervo TM. Corneal nerves: structure, contents and function. Exp Eye Res. 2003;76:521–542.

58. Brose K, Bland KS, Wang KH, Arnott D, Henzel W, Goodman CS, Tessier-Lavigne M, Kidd T. Slit proteins bind Robo receptors and have an evolutionarily conserved role in repulsive axon guidance. *Cell* 1999;96:795-806.

59. Hirst CE, Ng ES, Azzola L, Voss AK, Thomas T, Stanley EG, Elefanty AG. Transcriptional profiling of mouse and human ES cells identifies SLAIN1, a novel stem cell gene. *Dev Biol.* 2006;293:90-103.

60. Ma L, Tessier-Lavigne M. Dual branch-promoting and branch-repelling actions of Slit/Robo signaling on peripheral and central branches of developing sensory axons. *J Neurosci*. 2007;27:6843-6852.

61. Nguyen-Ba-Charvet KT, Brose K, Marillat V, Sotelo C, Tessier-Lavigne M, Checlotal A. Sensory axon response to substrate-bound Slit2 is modulated by laminin and cyclin GMP. *Mol Cell Neursci.* 2001;17:1048-1058.

62. González-Romero FJ, Gragera RR, Martínez-Murillo R, Martínez-Rodríguez R. Cytochemical and immunocytochemical comparative localization and characterization of acid sulfated glycolaminoglycans (sGAG) in several areas of the rat cerebral cortex during postnatal development. *J Hirnforsch.* 1994;35:511-20.

63. Schafer IA, Sorrell JM. Human keratinocytes contain keratin filaments that are glycosylated with keratan sulfate. *Exp Cell Res*. 1993;207:213-9.

64. Ohmori J, Nawa Y, Yang DH, Tsuyama S, Murata F. Keratan sulfate glycosaminoglycans in murine eosinophil-specific granules. *J Histochem Cytochem.* 1999;47:481-488.

65. Nakamura H, Hirata A, Tsuji T, Yamamptp T. Immunolocalization of keratan sulfate proteoglycan in rat calvaria. *Arch Histol Cytol*. 2001;64;109-118.

66. Cohen RJ, Holland JW, Redmond SL, McNeal JE, Dawkins HJS. Identification of the glycosaminoglycan keratan sulfate in the prostatic secretory cell. *The Prostate* 2000;44:204-209.

67. Marson A, Robinson DE, Brookes PN, et al. Development of a microtiter plate-based glycosaminoglycan array for the investigation of glycosaminoglycan-protein interactions. *Glycobiology* 2009;19:1537-1546.

68. Wang DN, Liu SY, Trummer BJ, Deng C, Wang AL. Carbohydrate microarrays for the recognition of cross-reactive molecular markers of microbes and host cells. *Nat Biotech*. 2002;20:275-281.

69. Saito A, Munakata H. Factor H is a dermatan sulfate-bidning protein: identification of a dermatan sulfate-mediated protease that cleaves factor H. *J Biochem* 2005;137:225-233.

70. Marson A, Rock MJ, Cain SA, Freeman LJ, Morgan A, Mellody K, Shuttleworth CA, Baldock C, Kielty CM. Homotypic fibrillin-1 interactions in microfibril assembly. *J Biol Chem.* 2005;278:41205-41212.

71. Yang B, Yang BL, Goetinck PF. Biotinylated hyaluronic acid as a probe for identifying hyaluronic acid-binding proteins. *Anal Biochem* 1995;228:299-306.

72. Parkar AA, Day AJ. Overlapping sites on the Link module of human TSG-6 mediate binding to hyaluronan and chondroitin 4-sulfate. *FEBS LETTERS* 1997;410:413-417.

73. Watanabe H, Cheung SC, Itano N, Kimata K, Yamata Y. Identification of hyaluronan-bindig domains of aggrecan. *J Biol Chem.* 1997;272:28057-28065.

74. Laterra J, Culp LA. Differences in the hyaluronate binding to plasma and cell surface fibronectins: requirement for aggregation. *J. Biol Chem.* 1982:257;719-726.

75. Arai T, Busby W, Clemmons DR. Binding of insulin-like growth factor (IGF) I or II to IGF-binding protein-2 enables it to bind to heparin and extracellular matrix. *Endocrin* 1996;11:4571-4575.

76. Nadesalingam J, Bernal AL, Dadds AW, Willis AC, Mahoney DJ, Day AJ, Reid KBM, Palaniyar N. Identification and characterization of a novel interaction between pulmonary surfactant protein D and decorin. *J Biol Chem.* 2003;278:25678-25687.

77. Mahoney DJ, Mulloy B, Forster MJ, Blundell CD, Fries E., Milner CM, Day AJ. Characterization of the interaction between tumor necrosis factor-stimulated gene-6 and heparin: implications for the inhibition of plasmin in extracellular matrix microinvironments. *J Biol Chem* 2005;280:27044-27055.

78. Harris EN, Weigel JA, Weigel PH. The human hyaluronan receptor for endocytosis (HARE/Stabilin-2) is a systemic clearance receptor for heparin. *J Biol Chem* 2008;283:17341-17350.

79. Boucas RI, Trindade ES, Tersariol IL, Dietrich CP, Nadar HB. Development of an enzyme-linked immunosorbant assay (ELIZA)-like fluorescence assay to investigate the interactions of glycosaminoglycans to cells. *Anal Chim Acta* 2008;618:218-226.

80. Zhang F, McLellan JS, Ayala AM, Leahy DJ, Linhardt RJ. Kinetic and structural studies on intereactions between heparin or heparan sulfate and proteins of the Hedgehog signaling pathway. *Biochemistry* 2007;46:3933-3941.

81. Tai G-H, Nieduszynski IA, Fullwood NJ, Huckerby TN. Human Corneal Keratan Sulfates. *J Biol Chem,* 1997;272:28227-28231.

82. Achur RN, Muthusamy A, Madhunapantula SV, Bhavanandan VP, Seudieu C, Gowda DC. Chondroitin sulfate proteoglycans of bovine cornea: structural characterization and assessment for the adherence of *Plaqsmodium faciparum*-infected erythrocytes. *Biochim Biophsy Acta* 2004;1701:109-119.

83. Plaas AH, West LA, Thonar EJA, Karcioglu ZA, Smith CJ, Klintworth GK, Hascall VC. Altered fine structure of corneal and skeletal keratan sulfate and chondroitin/dermal sulfate in macular corneal dystrophy. *J Biol Chem.* 2001;276:39788-39796.

84. Achur RN, Kakizaki I, Goel S, Kojima K, Madhunapantula SV, Goyal A, Ohta M, Kumar S, Takagaki K, Gowda DC. Structural interactions in chondroitin 4-sulfate mediated adherence of *Plasmodium falciparum* infected erythrocytes in human placenta during pregnancy-associated malaria. *Biochemistry* 2008;47:12635-12643.

85. Gama CI, Tully SE, Sotogaku N, Clark PM, Rawat M, Vaidehi N, Goddard WA, Nishi A, Hsieh-Wilson LC. Sulfation patterns of glycosaminoglycans encode molecular recognition and activity. *Nature Chem Biol.* 2006;2:467-473.

86. Hileman RE, Fromm JR, Weiler JM, Linheardt RJ. Glycosaminoglycan-protein interactions: definition of consensus sites in glycosaminoglycan binding proteins. *BioEssays* 1998;20:156-167.

87. Salamat-Miller N, Fang J, Seidel CW, Smalter AM, Assenov Y, Albrecht M, Middaugh CR. A network-based analysis of polyanion-binding proteins utilizing yeast protein arrays. *Mol Cell Proteomics* 2006;5:2263-2278.

88. Salamat-Miller N, Fang J, Seidel CW, Assenov Y, Albrecht M, Middaugh CR. Anetwork-based analysis of polyanion-binding proteins utilizing human protein arrays. *J Biol Chem.* 2007;282:10153-10163.

89. Jones LS, Yazzie B, Middaugh CR. Polyanions and the proteome. *Mol Cell Proteomics* 2004;3:746-769.

90. Wright PE, Dyson HJ. Intrinsically unstructured proteins: re-assessing the protein structure-function paradigm. *J Mol Biol.* 1999;293:321-331.

91. Hanks SK, Quinn AM. Protein kinase catalytic domain sequence database: Identification of conserved features of primary structure and classification of family members. *Methods Enzymol.* 1991;200:38-62.

92. Rogers MA, Langbein L, Winter H, Ehmann C, Praetzel S, Schweizer J. Characterization of a first domain of human high glycine-tyrosine and high sulfur keratin-associated protein (KAP) genes on chromosome 21q22.1. *j Biol Chem.* 2002;277:48993-49002.

93. Wu A, Chen J, Baserga R. Nuclear insulin receptor substrate-1 activates promoters of cell cycle progression genes. *Oncogene* 2008;27:397-403.

94. Araki E, Sun XL, Haag BL, Chuang LM, Zhang Y, Yang-Feng TL, White MF, Kahn CR. Human skeletal muscle insulin receptor substrate-1. Characterization of the cDNA, gene, and chromosomal localization. *Diabetes*, 1993;42:1041-1054.

95. Li HS, Chen JH, Wu W, Fagaly T, Zhou L, Yuan W, Dupuis S, Jiang ZH, Nash W, Gick C, Ornitz DM, Wu JY, Rao Y. Vertebrate slit, a secreted ligand for the transmembrane protein roundabout, is a repellent for olfactory bulb axons. *Cell* 1999;96:807–818.

96. Wang KH, Brose K, Arnott D, Kidd T, Goodman CS, Henzel W, Tessier-Lavigne M. Biochemical purification of a mammalian slit protein as a positive regulator of sensory axon elongation and branching. *Cell.* 1999;96:771-784.

97. Liang Y, Annan RS, Carr SA, Popp S, Mevissen M, Margolis RK, Margolis RU. Mammalian homologues of the *Drosophila* Slit protein are ligands of the heparan sulfate proteoglycan glypican-1 in brain. *J Biol Chem.* 1999;274:17885-17892.

98. Ronca F, Anderson JS, Paech V, Margolis RU. Characterization of Slit protein interactions with Glypican-1. *J Biol Chem.* 2001;276:29141-29147.

99. Edwards KL, Kueltzo LA, Fisher MT, Middaugh CR. Complex effects of molecular chaperones on the aggregtion and refolding of fibroblast growth factor-1. *Arch Biochem Biophys* 2001;393:14-21.

100. Park SM, Jung HY, Kim TD, Park JH, Yang CH, Kim J. Distinct roles of the N-terminal-binding domain and the C-terminal-solubilizing domain of alpha-synuclein, a molecular chaperone. *J Biol Chem.* 2002;277:28512-28520.

101. Hingorani K, Szebeni A, Olson MO. Mapping the functional domains of nucleolar protein B23. *J Biol Chem.* 2000;275:24451-24457.

Figure Legends

Figure 1. SPR sensorgrams of SLIT2−KS interactions. From top to bottom, concentrations of SLIT2 were 150, 130, 70, 50, 20, 10 nM, respectively.

Figure 2. SLIT2 binds to KS in a concentration-dependent and saturable manner with a logarithmic trend line.

Table 1: Protein Epitopes used in Nerve-related Protoarray:

Protein	Symbol	w IgG_1	w/o IgG_1
Human IgG_1 Pro100-Lys330		X	
Human Integrin alpha V beta 3	αVβ3		#
Human Integrin alpha 3 beta 1	α3β1		#
Human FGF acidic	FGFa		#
Human FGF basic (157 aa),	FGFb		#
Human EGF	EGF		#
Human PDGF	PDGF		#
Human TGF-beta 1	TGFβ1		#
Human NT-3	NT3		#
Human TrkA	Ntrk1	X	X
Human TrkB	Ntrk2		#
Human TrkC	Ntrk3	X	X
Human NGFR/TNFRSF16	NGFR		X
Human Neuregulin-1, SMDF isoform	NRG1		#
Human ErbB2	ERBB2	X	X
Human ErbB4	ERBB4	X	X
Mouse SLIT3	SLIT3		#
Rat ROBO1	ROBO1	X	X
Human ROBO2	ROBO2	X	X
Mouse Ephrin-A1	EFNA1	X	X
Mouse Ephrin-A2	EFNA2	X	X
Human Ephrin-A3	EFNA3	X	X
Human Ephrin-A4	EFNA4	X	X
Human Ephrin-A5	EFNA5	X	X
Mouse Ephrin-B1	EFNB1	X	X
Mouse Ephrin-B2	EFNB2	X	X
Human Ephrin-B3	EFNB3	X	X
Human EphA1	EPHA1	X	X
Mouse EphA2	EPHA2	X	X
Mouse EphA3	EPHA3	X	X
Mouse EphA4	EPHA4	X	X
Rat EphA5	EPHA5	X	X
Mouse EphA6	EPHA6	X	X
Mouse EphA7	EPHA7	X	X
Mouse EphA8	EPHA8	X	X
Rat EphB1	EPHB1	X	0
Mouse EphB2	EPHB2	X	X
Mouse EphB3	EPHB3	X	0

Mouse EphB4	EPHB4	X	X
Mouse EphB6	EPHB6	X	X
Human Semaphorin 3A	SEMA3A	X	0
Human Semaphorin 3E	SEMA3E		#
Mouse Semaphorin 3F (Trunc)	SEMA3F	X	X
Human Semaphorin 4A	SEMA4A	X	0
Human Semaphorin 6A	SEMA6A	X	X
Human Semaphorin 6B	SEMA6B	X	X
Human Neuropilin-1	NPN1		#
Human Neuropilin-2	NPN2	X	X
Chicken Netrin-1	NTN1		#
Chicken Netrin-2	NTN2		#
Human Netrin-4	NTN4		#
Mouse DCC	DCC	X	
Rat UNC5H1	UNC5H1	X	
Rat UNC5H2	UNC5H2	X	
Human UNC5H3	UNC5H3	X	
Human UNC5H4	UNC5H4	X	

X=incorporated in protoarray.
#=incorporated in protoarray; only available without IgG1 fusion.
0=no IgG_1 cleaved form available.
Total Number of Proteins=85

Table 2: Proteins that Interact with Highly Sulfated Keratan Sulfate GAG Chains [217/8268]

Protein	Signal	Database ID	Invitrogen ID	Protein Description
ABL1	43459	NP_005148.2	P3049	v-abl Abelson murine leukemia viral oncogene homologue 1
DNAJC8	41722	NP_055095.2	NM_014280.1	DnaJ (Hsp40) homologue, subfamily C, member 8
PQBP1	39994	NP_005701.1	NM_005710.1	Polyglutamine binding protein 1
ABL1	38005	NP_005148.2	PV3864	v-abl Abelson murine leukemia viral oncogene homologue 1, E255K
RPS6KB2	37356	NP_003943	PV3831	Ribosomal protein S6 kinase, 70kDa, polypeptide 2
TBK1	37330	NP_037386.1	PV3504	TANK-binding kinase 1
PLK1	36949	NP_005021.2	PV3501	Polo-like kinase 1 (Drosophila)
ABL1	36821	NP_005148.2	PV3866	v-abl Abelson murine leukemia viral oncogene homologue 1, T351I
CAPRIN1	35834	NP_005889.3	NM_005898.4	Cell cycle associated protein 1
COL23A1	35723	NP_775736.2	BC042428.1	Collagen, type XXIII, alpha 1
ABL1	35400	NP_005148.2	PV3865	v-abl Abelson murine leukemia viral oncogene homologue 1, G250E
AXL	35361	NP_068713	PV3971	AXL receptor tyrosine kinase
NUAK1	35266	NP_055655.1	PV4127	NUAK family, SNF1-like kinase 1
ABL1	38005	NP_005148.2	PV3863	v-abl Abelson murine leukemia viral oncogene homologue 1, Y253F
PDAP1	34768	NP_055706	NM_014891.1	PDGFA associated protein 1
AFF4	34570	NP_055238.1	BC025700.1	AF4/FMR2 family, member 4
CCDC43	34393	NP_653210	BC047776.2	Coiled-coil domain containing 43
EPB49	34349	NP_001107608	BC052805.1	Dematin: erythrocyte membrane protein band 4.9
CHUK	34299	NP_001269	PV4310	Conserved helix-loop-helix ubiquitous kinase
F11R	34234	NP_058642.1	NM_016946.3	F11 receptor
CDC2	34115	NP_001777.1	PV3292	Cell division cycle 2, G1 to S and G2 to M
MYLK2	32835	NP_149109.1	PV3757	Myosin light chain kinase 2, skeletal muscle
RAD51AP1	32494	NP_006470.1	NM_006479.2	RAD51 associated protein 1
CCNT1	32383	NP_001231	PV4131	Cyclin T1
KCNAB2	32108	NP_003627.1	NM_003636.1	Potassium voltage-gated channel, shaker-related subfamily, beta 2
KIT V654A	31817	NP_000213	PV4132	v-kit Hardy-Zuckerman 4 feline sarcoma viral oncogene homologue
DIDO1	31785	NP_149072.1	BC000770.1	Death inducer-obliterator 1
RPS6KA1	31745	NP_002944.2	PV3680	Ribosomal protein S6 kinase, 90kDa, polypeptide 1
CCDC55	31679	NP_115517.1	NM_032141.1	Coiled-coil domain containing 55
ADD2	31550	NP_059522.1	BC065525.1	Adducin 2 (beta)
PRR15	31499	NP_787083	NM_175887.2	Proline rich 15
BTK	31423	NP_000052	PV3363	Bruton agammaglobulinemia tyrosine kinase
ITGA6	31406	NP_000201.2	NM_000210.1	Integrin alpha 6
PHF15	31163	NP_056103	BC00492.1	PHD finger protein 15
UBE2S	31160	NP_055316	BC004236.2	Ubiquitin-conjugating enzyme E2S
RPS6KA2	30817	NP_066958.2	PV3846	Ribosomal protein S6 kinase, 90kDa, polypeptide 2
STK25	30743	NP_006365.2	PV3657	Serine/threonine kinase 25 (STE20 homologue, yeast)
HSPC148	30545	NP_057487.2	BC040946.1	CWC 15 homologue (S. cerevisiae)
MAP2	30395	NP_002365.3	NM_031845.1	Microtuble-associated protein 2
NTRK3	30375	NP_002521	PV3617	Neurotrophic tyrosine kinase, type 3
BMX	30146	NP_001712	PV3371	BMX non-receptor tyrosine kinase
NEK2	29418	NP_002488	PV3360	NIMA (never in mitosis gene a)-related kinase 2
NEK3	29363	NP_689933	PV3821	NIMA (never in mitosis gene a)-related kinase 3
ARHGAP17	29340	NP_001006635.1	NM_001006634.1	Rho GTPase activating protein 17
DAPK2	29080	NP_055141.2	PV3614	Death-associated protein kinase 2
MAP2K2	29037	NP_109587.1	PV3615	Mitogen-associated protein kinase kinase 2

UBXD3	28418	NP_689589	NM_152376.2	UBX domain containing 3
PAK4	28292	NP_005875.1	NM_005884.2	p21(CDKN1A)-activated kinase 4
ANKRD50	27779	NP_065070	BC024725.1	Ankyrin repeat domain 50
ABL2	27620	NP_009298.1	PV3266	v-abl Abelson murine leukemia viral oncogene homologue 2
CACNB1	27417	NP_000714.3	NM_000723.3	Calcium channel, voltage-dependent, beta 1 subunit
TSSK2	27281	NP_443732.3	PV3622	Testis-specific serine kinase 2
SCEL	27277	NP_659001.1	BC020726.1	Sciellin
SERBP1	27009	NP_001018077.1	BC003049.1	SERPINE1 mRNA binding protein
RPS6KA4	26944	NP_003933	PV3782	Ribosomal protein S6 kinase, 90kDa, polypeptide 4
TBC1D10C	26829	NP_940919.1	NM_198517.2	TBC1 domain family, member 10C
KIAA1706	26773	NP_085139.2	NM_030636.1	KIAA1706 protein
WIBG	26756	NP_115721.1	NM_032345.1	Within bgcn homologue (Drosophila)
E2F8	26667	NP_078956.2	BC028244.1	E2F transcription factor 8
FKBP3	26667	NP_002004	NM_002013.2	FK506 binding protein 3
TCEAL2	26595	NP_525129	NM_080390.3	Transcription elongation factor A (SII)-like 2
VRK3	26225	NP_057524.3	NM_016440.1	Vaccinia related kinase 3
AURKB	25925	NP_004208.2	PV3970	Aurora kinase B
STK24	25564	NP_003567.2	PV3560	Serine/threonine kinase 24 (STE20 homologue, yeast)
CSNK1G2	25425	NP_001310.3	PV3499	Casein kinase 1, gamma 2
DAPK3	25279	NP_001339	PV3686	Death-associated protein kinase 3
DCX	25123	NP_835365.1	NM_178152.1	Doublecortin: Doublecortex; lissencephaly, X-linked
SMITH	25068	NP_066972.1	Smith	SMITH antigen (Sm)
SCYE1	24980	NP_001135887.1	BC01451.1	Small inducible cytokine subfamily E, member 1, endothelial monocyte activating
PRKG2	24956	NP_006250.1	PV3973	Protein kinase, cGMP-dependent, type II
PRR16	24762	NP_057728.1	BC038838.1	Proline rich 16
DDX42	24754	NP_031398.2	BC015505.1	DEAD (Asp-Glu-Ala-Asp) box polypeptide 2
NEK4	24659	NP_003148.2	PV4315	NIMA (never in mitosis gene a)-related kinase 4
TTK	24534	NP_003309.2	PV3792	TTK protein kinase
WWP2	24484	NP_008945.2	BC000108.1	WW domain containing E3 ubiquitin protein ligase 2
ARPP-19	24474	NP_006619.1	NM_006628.4	Cyclic AMP phosphoprotein, 19kD
CSNK1E	24328	NP_001885.1	PV3500	Casein kinase 1, epsilon
ABLIM1	24223	NP_002304.3	BC002448.2	Actin binding LIM protein 1
MAP2K6	24152	NP_002749.2	PV3318	Mitogen-associated protein kinase kinase 6
PAK1	23993	NP_002567	PV3820	p21/Cdc42/Rac1-activated kinase 1 (STE20 homologue, yeast)
ANKS4B	23921	NP_665872.2	NM_145865.1	Ankyrin repeat and sterile alpha motif domain containing 4B
DCAMKL2	23892	NP_689832	PV4297	Doublecortin and CaM kinase-like 2
ZNF706	23792	NP_057180.1	NM_016096.1	Zinc finger protein 706
IRS1	23732	NP_005535.1	BC053895.1	Insulin receptor substrate 1
FAM128A	23684	NP_001078834.1	BC018206.1	Family with sequence similarity 128, member A
ACTR1B	23582	NP_005726.1	NM_005735.2	Centractin beta (yeast): actin-related protein homologue B
KIAA1143	23465	NP_065747.1	BC016790.1	KIAA1143
CTNNA1	23428	NP_001894.2	BC031262.1	Catenin (cadherin-associated protein), alpha 1, 102kDa
EPHA2	23315	NP_004422.2	PV3688	Ephrin receptor A2
HOMER2	23290	NP_004830.2	BC012109.1	Homer homologue 2 (Drosophila)
NTRK2	23143	NP_006171	PV3616	Neurotrophic tyrosine kinase, receptor, type 2
TCP10L	23126	NP_653260.1	NM_144659.1	t-complex 10 (mouse)-like
LIMCH1	22817	NP_055803.2	BC023546.2	LIM and calponin homology domains 1
YES1	22580	NP_005424.1	P3078	v-yes-1 Yamaguchi sarcoma viral oncogene homologue 1
EIF5	22457	NP_001960.2	BC032866.2	Eukaryotic translation initiation factor 5

KIF2C	22401	NP_006836.2	BC014924.1	Kinesin family member 2C
EIF3S4	22358	NP_003746.2	BC014924.1	Eukaryotic translation initiation factor 3, subunit G
SRPK1	22335	NP_003128.3	PV4215	SFRS protein kinase 1
TRPT1	22333	NP_113660.1	NM_031472.1	tRNA phosphotransferase 1
SMTNL2	22279	NP_940903.2	NM_198501.1	Smoothelin-like 2
LARP4	22254	NP_954658.1	NM_199188.1	La ribonucleoprotein domain family, member 4
NMT1	22231	NP_066565.1	NM_021079.2	N-myristoyltransferase 1
DAP	22223	NP_004385.1	NM_004394.1	Death-associated protein
MAPRE1	22209	NP_036457.1	NM_012325.1	Microtubule-associated protein, RP/EB family, member 1
CSNK1G3	22208	NP_004375.2	PV3838	Casein kinase 1, gamma 3
NTRK1	22192	NP_002520.2	PV3134	Neurotrophic tyrosine kinase, receptor, type 1
KIF3B	22121	NP_004789.1	NM_004798.2	Kinesin family member 3B
EBAG9	21974	NP_004206.1	NM_004215.2	Estrogen receptor binding associated, antigen 9
FGFR1OP	21817	NP_008976.1	NM_007045.2	FGFR1 oncogene partner
NPM1	21797	NP_002511.1	BC021983.1	Numatrin: nucleophosmin (nucleolar phoshoprotein B23)
LARP6	21777	NP_060827.2	NM_018357.2	La ribonucleoprotein domain family, member 6
LYN	21548	NP_002341.1	P2907	v-yes-1 Yamaguchi sarcoma viral oncogene homologue
RTF1	21542	NP_055953.3	NM_105138.2	Rtf1, Paf1/RNA polymerase II complex component, homolog
FES	21524	NP_001996.1	PV3354	Feline sarcoma oncogene
HMGB1	21497	NP_002119.1	NM_002128.2	High-mobility group box 1
SLC4A1AP	21473	NP_060628.2	NM_018158.1	Solute carrier family 4 (anion exchanger) member 1, adaptor protein
NMT2	21461	NP_004799.1	BC006376.1	N-myristoyltransferase 2
G3BP1	21423	NP_938405.1	NM_198395.1	GTPase activating protein (SH3 domain) binding protein 1
IRAK4	21417	NP_057207	PV3362	Interleukin-1 receptor-associated kinase 4
PSRC1	21391	NP_116025.1	NM_032636.2	Proline/serine-rich coiled-coil 1
RBM8A	21196	NP_005096.1	NM_005105.2	RNA binding motif protein 8A
EPHA8	21107	NP_065387	PV3844	Ephrin receptor A8
LMNA	21093	NP_733821.1	BC033088.1	Lamin A/C
SYTL2	20914	NP_116561.1	NM_032943.2	Synaptotagmin-like 2
TSSK1B	20661	NP_114417	PV3505	Testis-specific serine kinase 1B
RGS14	20566	NP_006471.2	NM_006480.4	Regulator of G-protein signaling 14
AURKA	20210	NP_940839	PV3612	Aurora kinase A
NKIRAS1	19916	NP_065078.1	NM_020345.3	NFKB inhibitor interacting RAS-like 1
PPID	19915	NP_005029.1	NM_005038.1	Cyclophilin D: peptidylprolyl isomerase D
MARK4	19852	NP_113605	PV3851	MAP/microtubule affinity-regulating kinase 4
NEK1	19713	NP_006613	PV4202	NIMA (never in mitosis gene a)-related kinase 1
LENG1	19379	NP_077292.1	NM_024316.1	Leukocyte receptor cluster member 1
SETBP1	19196	NP_056374.2	BC062338.1	SET binding protein 1
PPP1R8	19041	NP_054829.2	NM_014110.3	Protein phosphatase 1, regulatory (inhibitor) subunit 8
CFDP1	18952	NP_006315.1	NM_006324.1	Craniofacial development protein 1
DDX19B	18769	NP_009173.1	NM_007242.3	DEAD (Asp-Glu-Ala-Asp) box polypeptide 19B
ZAK	18704	NP_598407	PV3882	Sterile alpha motif and leucine zipper containing kinase AZK
ASXL1	18629	NP_056153.2	BC064984.1	Additional sex-combs like 1 (Drosophila)
FGFR1	18588	NP_000595	PV3146	Fibroblast growth factor receptor 1 (fms-related tyrosine kinase 2)
ERBB2	18556	NP_004439	PV3366	v-erb-b2; neuro/glioblastoma derived oncogene homologue (avian)
PTK2B	18455	NP_775266.1	BC036651.2	Protein tyrosine kinase 2 beta
DDX54	18433	NP_001104792.1	BC001131.1	DEAD (Asp-Glu-Ala-Asp) box polypeptide 54
MEOX1	18335	NP_004518.1	NM_004527.2	Mesenchyme homeobox 1
OCEL1	18291	NP_078854.1	NM_024578.1	Occludin/ELL domain containing 1

ING5	18217	NP_115705.2	NM_032329.4	Inhibitor of growth family, member 5
ASXL2	18195	NP_060733.4	BC042999.2	Additional sex-combs like 2 (Drosophila)
TFPT	18176	NP_037474.1	BC001728.1	TCF3 (E2A) fusion partner (in childhood leukemia)
IFRD2	18021	NP_006755.4	BC001327.1	Interferon-related developmental regulator 2
MARK2	17836	NP_059672.2	PV3878	MAP/microtubule affinity-regulating kinase 2
SIRPG	17784	NP_061026.2	BC064532.1	Signal-regulatory protein gamma
KDR	17770	NP_002244	PV3660	Kinase insert domain receptor (a type III receptor tyrosine kinase)
MRPL1	17755	NP_064621.3	BC015109.1	Mitochondrial ribosomal protein L1
RPAP3	17682	NP_078880.1	BC056415.1	RNA polymerase II associated protein 3
FAM50A	17629	NP_004690.1	NM_004699.1	Family with sequence similarity 50, member A
UBE2E2	17443	NP_689866.1	NM_152653.1	Ubiquitin-conjugating enzyme E2E 2
CDKN1B	17376	NP_004055.1	NM_004064.2	Cyclin-dependent kinase inhibitor 1B (p27, Kip1)
PKN2	17294	NP_006247	PV3879	Protein kinase N2
LIG3	17224	NP_039269.2	NM_013975.1	Ligase III, DNA, ATP-dependent
MESDC2	17222	NP_055969.1	BC012746.1	Mesoderm development candidate 2
TRUB1	17203	NP_631908.1	NM_139169.2	TruB pseudouridine (psi) synthetase homologue 1
MAPKAPK3	17148	NP_004626.1	BC001662.1	Mitogen-activated protein kinase-activated protein kinase 3
SRC	17080	NP_005408	P3044	v-src sarcoma (Schmidt-Ruppin A-2) viral oncogene homologue
BAIAP2	16925	NP_059344.1	BC014020.1	BAI1-associated protein 2
STAC	16897	NP_003140.1	BC020221.1	SH3 and cystein rich domain
TPPP	16891	NP_008961.1	NBM_007030.1	Tubulin polymerization promoting protein
FMNL1	16811	NP_005883.2	BC021906.1	Formin-like 1
HMGN1	16811	NP_004956.5	NM_004965.3	High-mobility group nucleosome binding domain 1
GLB1L	16727	NP_078782.3	NM_024506.3	Galactosidase, beta 1-like
FLT3	16478	NP_004110	PV3967	Fms-related tyrosine kinase 3
PIP4K2C	16448	NP_079055.3	NM_024779.2	Phosphotidylinositol-5-phosphaste 4-kinase, type II, gamma
GSK3B	16258	NP_002084	PV3365	Glycogen synthetase kinase 3 beta
ODF2	16221	NP_002531.3	BC010629.1	Outer dense fiber of sperm tails 2
ZHX2	16169	NP_055758.1	NM_014943.3	Zinc fingers and homeoboxes 2
DNM2	16068	NP_001005360.1	BC054401.1	Dynamin 2
LAD1	16058	NP_005549.2	NM_005558.2	Ladinin 1
COASY	16042	NP_001035994.1	BC020985.1	Coenzyme A synthetase
BRD3	15978	NP_031397.1	BC032124.1	Bromodomain containing 3
HCK	15939	NP_002101	P2908	Hemopoietic cell kinase
EFCAB4A	15902	NP_775855.3	BC033196.1	EF-hand calcium binding domain 4A
MAP3K10	15869	NP_002437	PV3877	Mitogen-activated protein kinase kinase kinase 10
BCAR3	15837	NP_003558.1	BC039895.1	Breast cancer anti-estrogen resistance 3
COIL	15815	NP_004636.1	NM_004645.1	Coilin
PCDHGC3	15791	NP_115779.1	NM_032403.1	Protocadherin gamma subfamily C, 3
EPHA3	15698	NP_005224	PV3359	Ephrin receptor A3
AMMECR1L	15601	NP_113633.2	NM_031445.1	AMME chromosomal region gene 1-like
ZMYM3	15595	NP_005087.1	BC013009.1	Zinc finger, MYM-type 3
SEMA3A-Fc	5913	NP_006071.1		Semasphorin 3A, extracellular domain

Table 3: CSA interaction with Invitrogen Proteins
[23/8268]

Protein	Signal	Accession #	Invitrogen ID	Protein Description
PLK1	64679	NP_005021	PV3501	Polo-like kinase 1 (Drosophila)
ITGA6	62823	NP_000201.2	NM_000210.1	Integrin, alpha 6, transcript varient 2
HADH	61418	NP_005318.2	BC000306.1	Hydroxyacyl-Coenzyme A dehydrogenase
KCNAB1	60955	NP_751892.1	NM_172160.1	Potassium voltage-gated channel, shaker-related subfamily, beta 1
NUDT16L1	60163	NP_115725.1	NM_032349.1	Nudix (nucleoside diphosphate linked moiety X)-type motif 16-1
CSNK1A1	59748	NP_001883	PV3850	Casein kinase 1, alpha 1
CHUK	54364	NP_001269	PV4310	Conserved helix-loop-helix ubiquitous kinase
COASY	47848	BC020985.1	BC020965.1	Coenzyme A synthase
KRTAP13-1	47443	NP_853630.2	NM_181599.1	Keratin associated protein 13-1
PAK1	39059	NP_002567	PV3820	p21/Cdc42/Rac1-activated kinase 1 (STE20 homologue, yeast)
RPS6KA5	38929	NP_004746.2	PV3681	Ribosomal protein S6 kinase, 90kDa, polypeptide 5
FLT1	37750	NP_002010	PV3666	Fms-related tyrosine kinase 1 receptor
MAP4K4	30089	NP_004825	PV3687	Mitogen-activated protein kinase kinase kinase kinase 4
KIAAA0515	29800	BC012289.1	BC012289.1	KIAAA0515
HOMER2	28772	NP_004830.2	BC01209.1	Homer homologue 2 (Drosophila)
GADD45GIP1	27379	NP_443082.2	BC013039.1	Growth arrest and DNA-damage-inducible gamma interacting prot.
CSNK1D	26494	NP_620693	PV3665	Casein kinase 1, delta
SLAIN2	26324	NP_065897.1	BC031691.2	SLAIN motif family, member 2
C11orf66	25433	NP_659454.1	BC053995.1	Chromosome 11, open reading frame 66
ACOX1	24045	NP_004026.2	BC010425.1	Acyl-coenzyme A oxidase 1, palmitoyl
PAK4	23005	NP_005875.1	NM_005884.2	p21(CDKN1A)-activated kinase 4
NUDT21	22423	NP_008937.1	NM_007006.1	Nudix (nucleoside diphosphate linked moietyX)-type motif 21
PLK1	19806	NP_005021	NM_005030.2	Polo-like kinase 1 (Drosophila)

Table 4: HA interaction with Invitrogen Proteins [6/8268]

Protein	Signal	Accession #	Invitrogen ID	Protein Description
KRTAP13-1	38193	NP_853630.2	NM_181599.1	Keratin associated protein 13-1
IRS1	14035	NP_005535.1	BC053895.1	Insulin receptor substrate 1
GFAP	4593	NP_002046.1	NM_002055.1	Glial fibrillary acidic protein
HADH	4296	NP_005318.2	BC000306.1	Hydroxyacyl-Coenzyme A dehydrogenase
LGALS8	2944	NP_006490.3	BC015818.1	Lectin, galactodsice-binding, soluble, 8 (galectin 8)
CABP4	2443	NP_660201.1	BC033167.1	Calcium binding protein 4

Table 5: KS interaction with Nerve-related Extracellular Molecules and Epitopes [40/85]

Protein	Signal	Accession #	Protein Description
SLIT3	41488	Q9WVB4	Mus Ser27-His901; secreted axon guidance factor; Robo ligand.
DCC-Fc	39177	NP_031857	Deleted in colorectal carcinoma, Mus Met1-Asn1097 + LINK+ HumIgG Pro100-Lys 330; attractive response toward netrin-1
ERBB4	33716	Q15303	Hum Glu26-Arg649. Type 1 glycoprotein, tyr protein kinase, & epidermal growth factor receptor.
SEMA3F-Fc	26174	QO88632	Mus Ala19-Pro775 + link + HumIgG Pro100-Lys 330. Secreted, sema domain, Ig domain, short basic domain, neuroguidance.
ERBB2-Fc	25936	NP_004439	Hum Thr23-Thr652 + Link + HumIgG Pro100-Lys 330; Type 1 glycopro, Tyr protein kinase & epidermal growth factor receptor.
EFNA3-Fc	19524	NP_004943.1	Ephrin A3 extracellular domain Hum(aa 1-209) + link + HumIgG Pro100-Lys 330; binds Eph receptors in developing neural tissue.
ROBO1-Fc	19284	O55005	Hum Met1-Ala16 + rat Lys 19-Lle 560 +link+HumIgG Pro100-Lys 330. Neural tissue negative Slit receptor.
EFNA1-Fc	16592	P52793	EphrinA1: Mus Asp19-Ser182 + link + HumIgG Pro100-Lys 330. Binds Eph receptors in developing neural tissue.
EFNB3-Fc	16459	NP_001397.1	EphrinB3: Hum Met1-Ser224 + Link + HumIgG Pro100-Lys 330. Binds Eph receptors in developing neural tissue.
EFNB1-Fc	14809	Q544L9	EphrinB1: Mus Lys30-Ser229 + Link + HumIgG Pro100-Lys 330. Binds Eph receptors in developing neural tissue.
EFNB2-Fc	13578	AAA82934	EphrinB2: Mus Arg27-Ala227 + Link + HumIgG Pro100-Lys 330. Binds Eph receptors in developing neural & angiogenic tissue.
EPHB4-Fc	13620	P54760	Eph B4: Mus Leu16-Ala539. Tyr kinase receptor, binds EFNB2 Inhibits cell-cell adhesion and angiogenesis.
SEMA6A-Fc	12914	NP_065847.1	Semaphorin6A: Hum Met1-Thr649 + Link + HumIgG Pro100-Lys 330. Anchored transmem signalling mol. Negative axon guidance.
EPHA1-Fc	12040	NP_005223.4	EphA1: Hum Met1-Glu547 + Link + HumIgG Pro100-Lys 330. Tyr receptor kin., binds EFNA1 in neuronal & angiogenic tissue.
EPHB3-Fc	10730	NP_034273.1	EphB3: Mus Met1-Thr530 + Link + HumIgG Pro100-Lys 330. Transmemb Tyr kinase receptor; binds EFNB1,-B2,-B3.
ROBO2-Fc	10188	NP_002933.1	Hum Met1-Ala312 + Link + Hum ROBO2 Pro313-Pro859 + HumIgG Pro100-Lys 330. Neural tissue negative Slit receptor. Permissive for neurite outgrowth via ROBO1-ROBO2 interaction.
SEMA3E	10117	O150041	Semaphorin3E: Mus Thr25-Ser775(Arg557Ala&Arg560Ala) secreted, axon &vascualr tip cell chemorepellant; binds Plexin.
ERBB4-Fc	9140	Q15303	HumGlu26-Arg649 + Link + HumIgG Pro100-Lys 330. Type I glycoprotein, tyr kinase & epidermal growth factor receptor.
SEMA3A-Fc	8203	Q14563	Semaphorin3A: Hum Lys26-Val771 + link + HumIgG Pro100-Lys 330. Secreted, binds nerve cell Neuropilin1+PlexinA receptor complex; neurorepellant.
EFNA2-Fc	8113	NP_031935.3	Mus Met1-Asn184 + Link + HumIgG Pro100-Lys 330. Binds EPH A2,-A3,-A4,-A5,-A6,-A7,-A8 receptors.Fcns in neuroguid.&angio
Ntrk3-Fc	7250	NP_002521	Neurotrophic tyrosine kinase, type 3; binds secreted NT-3.
EPHA8-Fc	7210	NP_031965.2	EphA8 Mus Met1-Arg540 + Link + HumIgG Pro100-Lys 330. Transmemb Tyr kinase receptor; binds EFNA5,-A3,-A3.

SEMA6A	7110	NP_065847.1	Semaphorin6A: Hum Met1-Thr649. Anchored transmembrane signalling molecule. Negative axon guidance.
NTN1	6956	AAC52971	Netrin1: Mus Val22-Ala603. Secreted neuroguidance molecule; interects with DCC, UNC5 family, & Neogenin receptors.
NRG1	6607	NP_039253.1	Human Neuregulin1, SMDF isoform, lacks Ig-like domain, trans-membrane domain, & cytoplasmic tail. Secreted neuroattractant.
SEMA6B-Fc	6607	Q9H3T3	Semaphorin6B: Hum CD33Met1-Ala16 + Hum Sem6B Leu26-Ser603 + Link + HumIgG Pro100-Lys 330. Type I glycoprotein w semaphorin domain. Binds Plexin4 w/o Neuropilin1; axon-repul.
EFNA5-Fc	6397	NP_001953.1	EphrinA5: Hum Met1-Asn203 + Link + HumIgG Pro100-Lys 330. Binds EPHsSA2-A8. Neurorepellant in neural tissue.
UNC5H2-Fc	5989	NP_071543.1	Rat Met1-Asp373 + Link + HumIgG Pro100-Lys 330. Transmem NTN receptor that mediates neurorepulsion with NTN1
EPHA6-Fc	5886	NP_031964.2	EphA6: Mus Met1-Gln546 + Link + HumIgG Pro100-Lys 330. Transmembrane EFN receptor.
NGFR-Fc	5833	NP_001057.1	Low Affinity Nerve Growth Factor Receptor: Hum p75 Met1-Asn250 + Link + HumIgG Pro100-Lys 330. Binds NGF, NT3,NT4
PDGFAB	5617	NP_036933.1 NP_113712.1	Dimerized Rat PDGFA Ser87-Aug196 & rat PDGFB Ser74-Thr 182. Binds to receptor kinases PDGF-α & PDGF-β.
EFNA4-Fc	5590	NP_031936.2	EphrinA4: Mus Met1-Gly176 + Link + HumIgG Pro100-Lys 330. Binds EPHA2-A7,-B1. Important in neurogenesis & angiogenesis.
EPHA7-Fc	5435	NP_001116361.1	EphA7: Mus Met1-Pro549 + Link + HumIgG Pro100-Lys 330. Tyrosine kinase receptor for EFNA1-A5. Neurogen. & angiogen.
NTN2	4894	Q90923	Netrin2: Chicken CD33 Met1-Met17 + Chicken NTN2 Ala16-Pro 581. Secreted neuroguidance molecule; interects with DCC, UNC5 family, & Neogenin receptors.
NTN4	4785	AAG53651	Netrin4: Hum Met1-Lys628. Secreted neuroguidance molecule; interects with DCC, UNC5 family, & Neogenin receptors.
EPHB1-Fc	4184	XP_001081949.1	EPHB1: Hum CD33 Met1-Ala16 + Rat EPHB1 Met18-Gln538 + Link+HumIgGPro100-Lys 330.Binds EFNA1,-A3,-A4,-B1,-B2,B3
EPHA3-Fc	3279	NP_034270.1	EphA3: Mus Met1-His541 + Link + HumIgG Pro100-Lys 330. Binds EFNA1-A5,-B1.
EPHA4-Fc	3014	NP_031962.2	EphA4: Mus Met1-Thr547 + Link + HumIgG Pro100-Lys 330. Binds EFNA1-A5,-B2,-B3.
SEMA4A-Fc	2996	NP_071762.2	Semaphorin4A: Hum Gly32-His 683 + Link + HumIgG Pro100-Lys 330. Transmembrane; fcns in immune & nervous tissue.
SEMA3F	2377	O88632	SemaphorinsF: Mus Ala19-Pro775(arg583Ala & Arg586Ala). Secreted, interacts with PlexinA3 & Neuropilin2, chemorepellant.

EFN As are GPI-membrane-anchored. EFN Bs are transmembrane.
Only membrane-bound or Fc-clustered ligands [Ephrins] can activate EPHs.

Table 6: CSA Interaction with Extracellular Nerve-Related Molecules and Epitopes [9/85]

Protein	Signal	Database ID	Protein Description
NTN4	7468	AAG53651	Netrin4: Hum Met1-Lys628. Secreted neuroguidance molecule.
UNC5H1-Fc	4515	NP_071542.1	Uncoordinated: Hum CD33 Met1-Ala16 + Rat UNC5H1 Gln26-Asp358). Receptor for secreted NTN axon guidance ligands.
SEMA6B-Fc	4264	Q9H3T3	Semaphorin6B: Hum CD33Met1-Ala16 + Hum Sem6B Leu26-Ser603 + Link + HumIgG Pro100-Lys 330. Transmembrane glycoprotein that fcns in neuroguidance.
EFNA3-Fc	4144	NP_004943.1	Ephrin A3 extracellular domain Hum(aa 1-209) + link + HumIgG Pro100-Lys 330; binds Eph receptors in developing neural tissue.
EPHA1-Fc	3062	P52793	EphrinA1: Mus Asp19-Ser182 + link + HumIgG Pro100-Lys 330. Binds Eph receptors in developing neural tissue.
DCC-Fc	2933	NP_031857	Deleted in colorectal carcinoma, Mus Met1-Asn1097 + LINK+ HumIgG Pro100-Lys 330; attractive response toward netrin-1
SEMA3E	2591	O150041	Semaphorin3E: Mus Thr25-Ser775(Arg557Ala&Arg560Ala) secreted, axon &vascualr tip cell chemorepellant; binds Plexin.
ROBO2-Fc	2546	NP_002933.1	Hum Met1-Ala312 + Link + Hum ROBO2 Pro313-Pro859 + HumIgG Pro100-Lys 330. Neural tissue negative Slit receptor.
EPHB2-Fc	2442	P29323	EphB2: Hum Met1-Leu543 + link + HumIgG Pro100-Lys 330. Transmembrane receptor; interacts with EFNA5 & EFNB ligands.

Table 7: Mimecan interaction with Invitrogen v4 Proteins [15/8268]

Protein	Signal	Accession #	Invitrogen ID	Protein Description
SLAIN2	50042	NP_065897.1	BC031691.2	SLAIN motif family, member 2
UBXD3	12008	NP_689589.1	NM_152376.2	UBX domain protein 3
DYRK3	9363	NP_003573	PV3837	Dual specificity serine/threonine and tyrosine kinase 3
APEX2	8757	NP_055296.2	NM_014481.2	Apurinic/apyrimidinic endonuclease 2, nuclear gene for mito prot.
MARK2	8389	NP_059672.2	PV3878	MAP/microtubule affinity-regulating kinase 2
CSNK1D	7668	NP_620693	PV3665	Casein kinase 1, delta (serine/threonine kinase)
AURKA	7657	NP_940839	PV3612	Aurora kinase A, serine/threonine, assoc. w centrosomes
KCNAB1	7601	NP_751891.1	NM_172159.2	Potasssium voltage-gated channel, shaker-related, beta 1
STK40	6187	NP_114406.1	NM_03217.1	Serine/thronine kinase 40
C11orf63	5318	NP_954575.1	NM_199124.1	Chromosome 11 orf 63, variant 2
PLK1	4143	NP_005021	PV3501	Polo-like kinase 1 (Drosophila) assoc w cell mitosis
TCP10L	3902	NP_653260.1	NM_144659.1	t-complex 10 (mouse)-like
KCNAB2	3808	NP_003627.1	NM_003636.1	Potassium voltage-gated channel, shaker-related subfamily, beta 2
CENK1E	3308	NP_001885	PV3500	Casein kinase 1, epsilon, assoc with DNA damage repair & cytokin
PAK6	2995	NP_064553	PV3502	p21(CDKN1A)-activated kinase 6, in testis & prostate.

Table 8. Langmuir 1**:**1 Binding Model Data for Interaction between SLIT2 and Biotinylated KS

	Keratan Sulfate
Ka × 10^{3} (M^{-1})	1.17 ± 0.24
Kd × 10^{-7} (s^{-1})	3.45 ± 2.37
K_D (nM)	27.77 ± 15.35

K_a: kinetic association rate constant
K_d: kinetic dissociation rate constant
K_D: Apparent equilibrium dissociation constant

Figure 1.

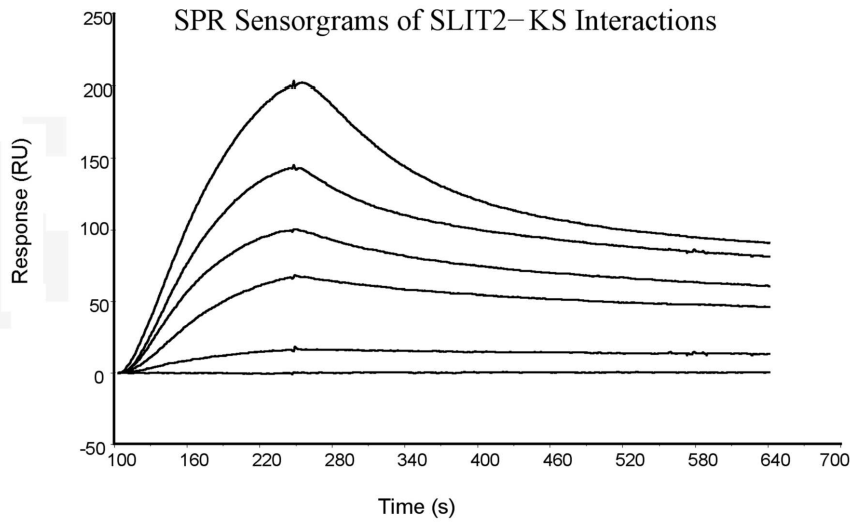

87x62mm (600 x 600 DPI)

Figure 2.

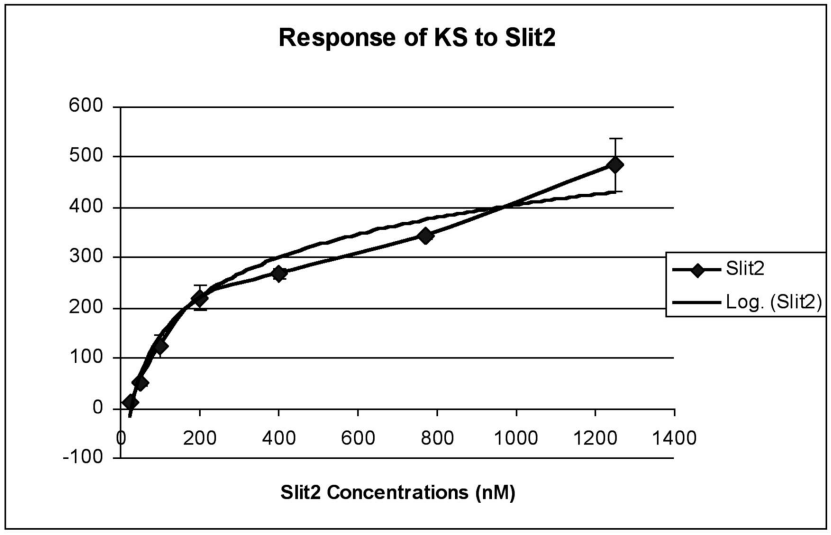

89x66mm (600 x 600 DPI)